NOTE TO USERS

This reproduction is the best copy available.

URBAN CHANGE DETECTION AND POPULATION PREDICTION MODELING USING MULTITEMPORAL LANDSAT TM IMAGES

By

HONGMEI ZHAO, B.Sc.

Nanjing Institute of Meteorology, China, 1986

A Thesis

Presented to Ryerson University

in Partial Fulfillment of the Requirements for

the Degree of Master of Applied Science

in the Program of Civil Engineering

Toronto, Ontario, Canada

DECLARATION

I, Hongmei Zhao, hereby declare that I am the sole author of this thesis.

I authorize Ryerson University to lend this thesis to other institutions or individuals for the purpose of scholarly research.

Hongmei Zhao
Department of Civil Engineering
Ryerson University

I further authorize Ryerson University to reproduce this thesis by photocopying or by other means, in total or in part, at the request of other institutions or individuals for the purpose of scholarly research.

Hongmei Zhao
Department of Civil Engineering
Ryerson University

BORROWER'S PAGE

Ryerson University requires the signature of all persons using or photocopying this thesis.

Please sign below, and give address and date.

Name of Borrowers	Date	Address	Signature

Urban Change Detection and Population Prediction Modeling Using Multitemporal Landsat TM Images

Hongmei Zhao,
Master of Applied Science, 2004
Department of Civil Engineering
Ryerson University

ABSTRACT

Urban environments belong to the most dynamic system on the earth's surface. Urban areas contain nearly half of the world's population. Understanding the growth and change brought on by urbanization is critical for urban planning, environmental studies, and resource management. This study is an attempt to present a satellite-based approach to modeling urban population growth from multitemporal and multispectral Landsat image data. The focus is placed on two aspects: detection of urban land cover changes and population prediction modeling associated with the urban expansion.

The study consists of an experimental set-up to generate the land cover maps and to recognize the vegetation-impervious surface-soil (V-I-S) patterns followed by integrating population census data and remote sensing data at the city planning district level. This is done in conjunction with geographic information systems (GIS) in order to model population growth from 1996 to 2001 in the City of Mississauga, Ontario. The main findings of this research show that a total of 81.6 km^2 of built-up areas have been added within Mississauga's boundaries between 1985 and 2002. This accounts for 25.5 % of the total area of Mississauga at the expense of non-built and water covered areas. The results show an increase of 6.5 % in built-up areas in the last three years (1999-2002), which results in an average growth rate of 7 km^2/year. The previous 14 years (1985-1999) have shown an increase of 19.0 % in development, which equals 4.3 km^2/year. The investigation also shows that a linear equation adequately describes the relationship between the population counts and the built-up area, or "C-442" area, of V-I-S components.

ACKNOWLEDGEMENTS

First of all, I would like to thank my supervisor, Prof. Dr. Jonathan Li, for his kind guidance and many good ideas. Special thanks for all of his fruitful discussions, invaluable suggestions and critical remarks. I would also like to thank him for introducing me to the active research fields of remote sensing and GIS. His serious and significant research has a great influence on my work. His efforts to ensure my financial support during my study are also appreciated.

I also attribute my accomplishments to Professors Dr. Michael A. Chapman, Dr. Songnian Li, and other faculty and staff members in the Department of Civil Engineering, for their encouragement. I would like to offer special thanks to Desmond Rogan for his technical assistance to solve computer and software-related problems. Many thanks are also extended to Leah Stanwyk, Kim Kritzer and Dianne Mendonca, for their administrative support.

I would like to acknowledge all my fellow graduate students at Ryerson University, who have helped me in countless ways and made the period of study an enjoyable time, in particular, Haibin Dong, Yu Li, Ruiqiu Li, Xiangqian Gao, Lijun Gu, Haibin Liu and Zheng Chang. I would like to express my gratitude to Kim Kritzer and Stéphane Lapointe, who spent time proofreading my thesis and correcting literal errors.

Financial support partially provided by the School of Graduate Studies is gratefully acknowledged. A special note of thanks is extended to Dr. Wayne Forsythe in the Department of Geography for his support in providing Landsat TM/ETM+ images used in my research.

Last, but not least, I wish to express my sincere appreciation to my parents, who provided unwavering encouragement, inspiration and support, and to my husband, Jianlin Lu and my son, Mike Lu, for their love, patience, help and understanding. They are the unsung heroes who gave their all without reservation to provide me the freedom to pursue my dreams. I would never have been able to succeed in my master's studies without their generous support.

TABLE OF CONTENTS

LIST OF FIGURES

LIST OF TABLES

LIST OF ABBREVIATIONS

ARSIS	Amelioration de la Résolution Spatiale par Injection de Structures
AVHRR	Advanced Very High Resolution Radiometer
CA	Composite Analysis
CMA	Census Metropolitan Area
CT	Census Tract
C-442	Combination of V-I-S area in a 40%, 40% and 20% ratio
EMR	Electro-Magnetic Radiation
ERTS-1	The firs Earth Resources Technology Satellite (later Landsat 1)
ETM+	Enhanced Thematic Mapper Plus
HRV	High Resolution Visible
HR VIR	High Resolution Visible Infra-Red
HSR	High Spectral Resolution
IFOV	Instantaneous Field of View (a measure of the area viewed by a single detector on a scanning system in a given instant in time)
ISODATA	Iterative Self-Organizing Data Analysis Technique
LULC	Land Use and Land Cover
MSS	Multi-Spectral Scanner
NAD83	North American Datum 1983
NDVI	Normalized Difference Vegetation Index
NIR	Near Infra-Red
MIR	Middle Infra-Red
MLC	Maximum Likelihood Classifier
NASA	National Aeronautics and Space Administration
PCA	Principal Component Analysis
SMA	Spectral Mixture Analysis
TM	Thematic Mapper
UTM	Universal Transverse Mercator
V-I-S	Vegetation-Impervious surface-Soil

Chapter 1

INTRODUCTION

1.1 Motivations

Urban environments are a part of a very vibrant system on Earth. Although city areas are relatively small in size, they accommodate nearly half of the world's population. Several decades of population explosion and accelerated urban growth have had profound environmental and socio-economic impacts felt in both developing and developed countries alike (Yang, 2003). This study is mainly motivated by the following factors.

First and foremost, the consequence of fast urban sprawl and dramatic population expansion induced many environmental challenges such as the green house effect, energy crises, water resources shortages, vegetation redistributions and potential agricultural failure. Urbanization has substantial influence on different aspects of the quality of life and has brought the extensive attention of researchers, urban planners, environmental monitors and landscape managers. In Canada, urbanization has been encouraged by the expansion or development of areas non-adjacent to the traditional downtown urban centers. These are the areas of emerging residential, commercial, and industrial development, thus encroaching on the forested and agricultural lands surrounding the city. Accurate and reliable information of land use/land cover (LULC) and population is required to quantify the current situation and to predict future trends. Unfortunately, conventional sources of information on both LULC and population are frequently

inadequate and are not updated regularly. There is a need to move beyond simply mapping the physical form of urban areas to provide indicators of their social and economic relations, such as with land-use and population density (Donnay et al., 2001).

Secondly, current approaches to urban change monitoring generally involve ground surveys and interpretation of aerial photographs, but these are expensive, time-consuming, and very difficult to implement on a regular mapping basis. Thus, fast and low-cost methods that are capable of automatically mapping urban areas are desired. Remote sensing techniques provide an excellent alternative means to meet this need. This approach is considered effective because of its inexpensiveness, efficiency, temporal consistency and spatial coverage. Along with the launch of high-resolution and multispectral optical satellites, more precise and reliable spatial images are obtained and updated in a timely manner to effectively support complex and dynamic urban environment monitoring. Furthermore, recent research interests in remote sensing applications have extended to many socio-economic issues, like pollution monitoring, disaster management, population growth prediction, urban heat island effect assessment, transportation planning, road safety analysis and so on.

Finally, despite many positive developments of remote sensing techniques, there are insufficient results regarding the potential for the operational application of remote sensing to map and monitor urban areas (Donnay, 1999) while most of the research efforts are put towards addressing the opportunities and problems posed by each new technological advance (Donnay et al., 2001).

Accordingly, the motivation of this study is to make use of digital satellite remotely sensed data to develop an operational solution to interpret, analyze and assess existing and will-be urban settlement characteristics. Based upon this, further display of its socio-economic impact can be achieved using remote sensing data coverage merging other spatial ancillary data types, such as, census data, GIS data, etc. (Nellis et al., 1990).

1.2 Problem Statement

1.2.1 Problem Definition

Mississauga, as a young city of the Greater Toronto Area (GTA), Ontario, has been experiencing rapid urban growth and population expansion. This is due to the acceleration of economic growth and the arrival of massive immigrant population since it was founded in 1974. According to Statistics Canada census data, the population of Mississauga had increased by 23.9%, 17.5%, 12.6%, from three different census periods in each five year interval from 1986 to 2001, respectively. Up to 2001, the population density reached 2,125 (people/km^2). There were about 612,925 people living in the City of Mississauga, which equals 1.6 times of its 1986 population (Statistics Canada, 2004; The Social Planning Council of Peel, 2004). Today, Mississauga is the sixth largest city in Canada with a rapid population growth of around 14,000 new residents per year.

This urban growth has a profound impact on the available water resources, agricultural land, energy consumption distribution and undeveloped land. Moreover, the ambitious plans of Mississauga project to accommodate a population of 780,000 by the middle of

the 21st century. This will result in a critical shortage of available space, as this growth rate largely relies on the supply of available land. The present fast economic and population expansion have exhausted most of its utilizable open space. Thus future growth is most likely to depend on the redevelopment and refill of existing built-up communities (City of Mississauga, 2004). Hence, the availability of spatiotemporal growth and land-cover change mapping are becoming essential in order to develop a sufficient infrastructure to sustain the growth (Gluch, 2002). This information will support future urban planning through establishing an input database of urban changes. Therefore, fully understanding Mississauga's urban change and population growth pattern, in its limited utilizable space, would enhance its development decision-making in the future.

1.2.2 Data Quality and Availability

Applicable and reasonable data sources are vital to ensure the implementation of the study objectives. Because of the widespread availability, frequency of update and cost, the focus of urban remote sensing research has shifted from traditional aerial photography to the use of digital multispectral satellite images (Donnay et al., 2001).

Since the launch of the world's first Earth Resources Technology Satellite (ERTS-1), later called Landsat-1, in 1972 by the U. S. National Aeronautics and Space Administration (NASA), the earth observation satellites have been experiencing continuous development. They have gone from coarse spatial resolution Landsat

Multispectral Scanner (MSS), Landsat Thematic Mapper (TM), to present medium resolution Enhanced Thematic Mapper Plus (ETM+) series, SPOT High Resolution Visible (HRV) series, to high-resolution IKONOS and QuickBird commercial imaging satellites. The spatial resolutions of the satellite data have been upgraded from the coarse resolution of 80m to medium resolution of 10-30m, and finally high-resolution of 0.6-5m. Among them, the U. S. Landsat and the French SPOT satellites are two major LULC mapping satellites. Landsat-7 ETM+ and SPOT-5 are providing the majority of remotely-sensed digital images in use today.

Coarse -to- Medium Resolution Satellite Imagery

Landsat satellites have provided high quality multispectral data since 1972. Over the past 30 years, there have been a total of seven Landsat satellites launched. Landsat -1, -2, and -3 are no longer in operation, while Landsat-6 suffered an early demise. Landsat-4 MSS and -5 TM were launched in 1982 and 1984, respectively, to collect MSS (approximately 80 m) with radiometric coverage in four spectral bands and TM data. Landsat 7, launched in April 1999, carries an Enhanced Thematic Mapper Plus (ETM+) sensor capable of providing medium-to-coarse resolution multispectral image data of the earths' surface (see Table 1.1). The TM sensor records the electromagnetic spectrum in seven bands with a spatial resolution of 28.5m for the visible, near-IR, and mid-IR wavelengths (six bands) and 120 m for one thermal-IR band. Landsat 7 ETM+ data is essentially the same as Landsat 5 TM data, except it has two distinct enhanced features: a new panchromatic band (Band 8) with 15 m spatial resolution, co-registered with the multispectral bands; and a thermal infrared band (Band 6) has increased resolution from previous 120m to

60m. In general, Landsat-4 and -5 data are noisier than the ETM+ data. Currently, only Landsat-5 and -7 are operational.

Table 1.1 Landsat-5 TM, Landsat-7 ETM+ and SPOT series characteristics

	Landsat TM/ETM+		SPOT	
	Band Width (μm)	Spatial Resolution (m)	Band Width (μm)	Spatial Resolution (m)
Band 1	0.45 - 0.52 (blue)	28.5 (TM) 30 (ETM+)	0.50 - 0.59 (green)	20 (SPOT 1,2,3,4) 10 (SPOT 5)
Band 2	0.52 - 0.60 (green)	28.5 (TM) 30 (ETM+)	0.61 - 0.68 (red)	20 (SPOT 1,2,3,4) 10 (SPOT 5)
Band 3	0.63 - 0.69 (red)	28.5 (TM) 30 (ETM+)	0.79 - 0.89 (NIR)	20 (SPOT 1,2,3,4) 10 (SPOT 5)
Band 4	0.75 - 0.90 (NIR)	28.5 (TM) 30 (ETM+)	1.58 - 1.73 (SNIR) (SPOT 4, 5)	20 (SPOT 4, 5)
Band 5	1.55 - 1.75 (NIR)	28.5 (TM) 30 (ETM+)		
Band 6	10.4 - 12.50 (thermal IR)	120 (TM) 60 (ETM+)		
Band 7	2.08 - 2.35 (middle IR)	30		
Panchromatic /Monospectral (SPOT 4,5)	0.52 - 0.90 (green-NIR)	15 (ETM+)	0.51 - 0.73 (SPOT 1,2,3) 0.61 - 0.68 (SPOT 4, 5)	10 (SPOT 1,2,3,4) 5 (SPOT 5)

The first SPOT imaging satellite (Satellite Pour l'Observation de la Terre) was launched in early 1986. There have been five SPOT satellites launched, providing medium-to-high resolution optical image data of the earth's surface over the visible (green and red) to near infrared portion of the electromagnetic spectrum. SPOT 1, 2 and 3 all carry two HRV (High Resolution Visible) sensors with multispectral (XS: Bands 1-3) and panchromatic (Pan) modes on board. SPOT 3 failed in November 1996. SPOT 4 and 5 both carry two HR VIR (High Resolution Visible Infrared) sensors and were successfully launched in

1998 and 2002, respectively. The HR VIR is similar to the HRV, except that HR VIR has an additional short-wavelength infrared (SWIR) band (XI4), and the narrower wavelength bandwidth of the panchromatic mode, also named as Monospectral (M) mode (Crisp, 2004) (see Table 1.1). The latest SPOT 5 combines a significant number of new and improved features over the previous sensors (Infoterra, 2004), such as better ground resolution (5m for panchromatic mode), higher resolution in multispectral mode (10m), repeat coverage every five days and High Resolution Stereoscopic (HRS) instrument providing simultaneous acquisition of stereo pairs (600 x 120 km) with an elevation accuracy of 10 m.

High-Resolution Satellite Imagery

Table 1.2 presents the main characteristics of the two types of high-resolution satellites currently in use. The world's first high-resolution commercial imaging satellite, IKONOS-2, was launched in September 1999 with a swath width of 11 km at nadir (Crisp, 2004). It delivers 1m resolution satellite imagery corresponding to anywhere in the world. IKONOS sensor records 4 channels of multispectral data at 4 m resolution and one panchromatic channel with 1 m resolution (Infoterra, 2004).

Another new generation of high-resolution commercial imaging satellite, QuickBird, was successfully launched in October 2001. This is currently the highest spatial resolution commercial imaging satellite available (see Table 1.2). QuickBird offers 0.6 m resolution panchromatic and 2.4m multispectral imagery. At 0.6 m resolution, buildings, roads, bridges and other detailed infrastructures become visible (Geocommunity, 2004).

Table 1.2 IKONOS and QuickBird characteristics.

	IKONOS		QuickBird	
	Band width (μm)	Spatial resolution (m)	Band width (μm)	Spatial resolution (m)
Band 1	0.45 to 0.53 (blue)	4	0.45 - 0.52 (blue)	2.44
Band 2	0.52 to 0.61 (green)	4	0.52 - 0.60 (green)	2.44
Band 3	0.64 to 0.72 (red)	4	0.63 - 0.69 (red)	2.44
Band 4	0.77 to 0.88 (NIR)	4	0.76 - 0.90 (NIR)	2.44
Panchromatic	0.45 to 0.90	1	0.45 – 0.90	0.61

Table 1.3 Summary of different data sources

Satellite sensor		Band	Spatial resolution (m)	Temporal resolution (day)	Radiometric resolution (bit)	Swath (km)	Orbit altitude (km)
Landsat series	1, 2, 3, 4 (MSS)	1-4	79	16	6 (0-63)	185*172	705
	5 ™	1-5,7	28.5	16	8 (0-255)	185*172	705
		6	120				
	7 (ETM+)	1-5,7	30	16	8 (0-255)	185*172	705
		6	60				
		8 (Pan)	15				
SPOT series	1, 2 (HRV)	(XS)1-3	20	26 (nadir) 1-3 (off-nadir)	8 (0-255)	60*60	832
		Pan	10				
	4 (HR VIR)	(XI)1-4	20	26 (nadir) 1-3 (off-nadir)	8 (0-255)	60*60	832
		Pan	10				
	5	(XI)1-4	10 (1-3) 20 (4)	5	8 (0-255)	60*60	832
		Pan	5				
IKONOS		1-4	4	1.5-3	11 (0-2047)	11*11	681
		Pan	1				
QuirckBird		1-4	2.44	1-3.5	11 (0-2047)	16.5*16.5	450
		Pan	0.61				

Comparison of Different Data Sources

Table 1.3 compares the different remote sensing data sources. The basic characteristics of data resources obtained from the satellites currently in use are summarized in this table according to their resolution, coverage, revisit time, etc.

1.2.3 Data Determination

Except for data quality and availability, data acquisition cost is a very important factor in urban change detection applications. Remote sensing data acquisition costs vary dramatically on a per unit basis. Generally, the older the data, the lower the per unit cost of acquisition will be (Lunetta, 1999).

Although the exact costs for remote sensing data acquisitions have fluctuated over the past decades, some relative cost relationships have remained consistent. The higher the spectral and spatial resolution, the more expensive the satellite data will be. Aerial photographs and ground survey involve more manpower, consequently costing more than digital satellite data. Table 1.4 is a cost comparison of different data sources (RADARSAT, 2004; SIMWRIGHT, 2004; USGS, 2004). The cost estimates are for simple general comparisons.

Taking into account data spatial resolution, availability and cost factor, the medium resolution satellite TM and ETM+ data are the most suitable for the actual application of

urban change detection at urban planning district level due to their inexpensive, long-run data series and timely update availability.

Table 1.4 Comparison of sensor's spatial and temporal resolution, coverage area, and approximate cost per unit area.

Sensor	Spatial Resolution (m)	Temporal Resolution (day)	Coverage/swath (km^2)	Unit cost US$/($km^2$)
Landsat MSS	79	16	31,820	0.006
Landsat TM	30	16	31,820	0.013
Landsat ETM+	30/15 (Pan)	16	31,820	0.019
SPOT 1-4	20/10 (Pan)	26 (nadir), 1-3 (off-nadir)	3,600	0.33/0.53
SPOT 5	10/5 (Pan)	5	3,600	0.94
IKONOS	4/1 (Pan)	1.5 - 3	121	25.2
QuickBird	2.44/0.61 (Pan)	1 - 3.5	272	24.0
Aerial photograph 1:40,000 Paper Print	0.3-0.9	Variable	83	16 (colour-IR) 10 (B&W)
Aerial photograph (Colour-IR) 1:40,000 Film Negative	0.3-0.9	Variable	83	24 (natural colour)

1.3 Research Objectives

As mentioned above, currently detailed and reliable information of urban changes and population is very crucial for urban planning, environment management, and decision-making, but are often not sufficiently available or updated. In comparison with the United

States, Canada has fallen behind in the field of urban change detection using applicable Landsat satellite data. The research literatures documented before 1993 (Martin et al., 1988; 1989; Gong et al., 1990; 1992; 1993) or after 2000 (Forsythe, 2004), and mainly focused on new strategy and technique investigations instead of addressing urban change implication.

In order to better understand the significant urban changes that have occurred in the last 20 years, and to better provide quantitative land cover change input data for urban planning and further applications in socio-economic aspect, a concrete investigation and identification of urban change is required. The focus of this study emphasizes the practical application of multitemporal Landsat TM/ETM+ data in urban land cover change detection and corresponding population growth modeling. The City of Mississauga is chosen as the study area due to its typical characteristics in urban change and population growth. Spanning the 30-year development, Mississauga has become the sixth largest city in Canada and an important economic pillar of the GTA, Ontario. The objective of this study is to provide a quantitative indicator of a rapidly expanding city in Canada by adopting an easy and applicable approach, which can then be applied in other cities using medium-resolution, multispectral and multitemporal Landsat TM/ETM+ data.

For the sake of clarity, land cover conversion is the focus of this study instead of land use change. Land cover refers to the type of feature physically present on the surface of the earth, while land use indicates the human activity or economic function associated with a

specific piece of land (Lillesand and Kiefer, 2000). The following tasks will be achieved in this study:

1) To generate classified land cover maps from multitemporal and multispectral Landsat TM/ETM+ images by means of post-classification approach.
2) To identify the two land cover features of built-up and non-built based on the reference data.
3) To determine areas of the urban growth according to comparison of classified land cover maps in different dates.
4) To recognize city change morphology based on the classified land cover maps using V-I-S model.
5) To carry out population prediction modeling analysis by integrating population counts and the classified output data of the pansharpened Landsat ETM+ image and resampled digital aerial othophoto in a GIS environment.

1.4 Structure of the Thesis

This thesis consists of six chapters. It has been delineated as follows:

Chapter 1 addresses the needs and the importance of using satellite image data for urban analysis. It gives a brief summary of the problem definition and overall objectives followed by a summary of the thesis structure.

Chapter 2 summarizes the state-of-the-art of land use/land cover classification and change detection techniques, V-I-S model and integration of remote sensing and GIS for

urban population prediction and analysis. It also outlines the issues encountered by utilizing these techniques and the need to integrate them.

Chapter 3 describes the study area and data sets used and the methodology applied in this study.

Chapter 4 presents the land cover change analysis results derived from image classification, and corresponding land cover change pattern identified by V-I-S model.

Chapter 5 depicts the population modeling results through the integration of resulting remote sensing data with population counts in a GIS environment.

Chapter 6 covers the thesis' concluding remarks and relevant recommendations for later research.

Chapter 2

LITERATURE REVIEW

Satellite remote sensing is defined as the science and technology of obtaining information from space about an object on the earth's surface through the analysis of data acquired by a satellite-borne sensor without direct contact with the object. It can be used to provide an objective and consistent view of urban areas in terms of required coverage and revisit capability (Lillesand et al., 2004). Multispectral, multisensor and high-resolution satellite imagery has further demonstrated satellite remote sensing's potential capability of collecting more precise and more detailed geospatial information. With the complicated and validated mathematical algorithms refinement, advanced image processing techniques are obtained to provide fundamental support to the further detection, mapping and monitoring of urban change details. This chapter summarizes the state-of-the-art of satellite-based techniques used for urban land cover and land use change detection and population estimation.

2.1 Satellite Remote Sensing for Urban Analysis: An Overview

Satellite imagery affords excellent means to monitor on-going and potential ecological threats and damages. As well, it monitors long term after effects to the earth's surface and to areas relevant to human activities (RST, 2004). In the 21st century, environmental issues have accepted unprecedented attention due to accelerated and unknown changes in the environment which can cause our socio-economic system unpredictable failure and

devastating consequences. Although many scientific discoveries have dramatically advanced our understanding of the ecosystem processed, predicting it with an acceptable degree of certainty is a challenge for humanity in the coming decades (Lunetta, 1999). Therefore, LULC mapping, land use pattern recognition and corresponding change detection are urgent and fundamental topics to be studied and answered. All the uncertainties of ecosystem changes happen on the basis of an accumulation of irregular environmental changes. The investigation of incidents lies directly in interpreting information derived from reality, such as weather change, soil erosion, vegetation deterioration, environmental contamination, drought and flooding occurrences, etc.

Phinn et al. (2002) summarized five current application themes of remote sensing in urban environments. They are (1) delimitation of LULC types; (2) assessment of the utility of texture measures to aid in separating urban LULC types(Gong and Howarth, 1990; 1992); (3) mapping areas of impervious and pervious surfaces for input into energy and moisture flux models; (4) mapping LULC changes in urban areas (Gong, 1993) and (5) application of empirical models to estimate biophysical, demographic and socio-economic variables (Forster, 1983; 1993; Jensen et al., 1994; Lo, 1997; Lo and Faber, 1997).

Ben-Dor (2001) concluded that remote sensing tools offer the capability of measuring both short- and long-term environmental change, but short-term aspects call for a more sensitive methodology for tracking small, visual, chemical/physical changes that are expected over a short period of time. This is due to the high object-density of urban

scenes which cause problems such as shadowing and mixed-pixel effects. Ben-Dor stated that high spatial-resolution information from advanced orbital sensors is used more as a pattern recognition tool than as a source of information about the material's nature and composition. The solution is the use of sensors with high spectral-resolution capabilities, such as Hyperspectral Remote Sensing (HSR) technology.

In other words, as long as the real-time, accurate and dynamic remotely sensed imagery is available, instantaneously mapping, detecting and locating will, without doubt, be implemented using an effective interpretation and detection approach. The applications of remotely sensed satellite imagery have penetrated into different aspects of our daily life and there are too many application examples to be individually mentioned. This study will focus on substantial application of multitemporal Landsat images on urban change detection and population prediction modeling.

2.1.1 Existing Change Detection Techniques

Since the advent of the first Landsat satellite, research and development on algorithms of image interpretation and analysis has never stopped. Various imaging satellites ranging from Landsat to QuickBird create considerable challenges in terms of developing data-processing techniques to exploit information in urban scenes (Barnsley et al., 2001).These techniques are widely accepted conventional approaches established for coarse-to-medium resolution imagery, like Landsat MSS and TM data.

Change detection techniques can be broadly divided into either post-classification change detection or pre-classification spectral change detection (Lunetta, 1999). Land cover change detection can be accomplished using multidate satellite data through these two methods (Green et al., 1994; Yang and Lo, 2002; Yang et al., 2003).

In the post-classification approach, two images acquired from different dates are independently classified and labeled (Yang and Lo, 2002). The area of change is then extracted through the direct comparison of the classification results. This method is also named map-to-map comparison or classification-based method. Originally used for Landsat change detection in the late 1970s, it was considered to be the most reliable and was used as a standard for quantitative evaluation of emerging image differencing techniques (Weismiller et al., 1977). An important advantage of this method is that data normalization is not required because the two dates are classified separately (Singh, 1989). For many applications, the map-to-map comparison is preferred as it can detect a full matrix of LULC changes (Charbonneau et al., 1993; Jensen et al., 1995; Miller et al., 1998). The data sources of Landsat MSS and TM, SPOT HRV are favored for urban LULC change mapping, as they have a long period of operation (Yang and Lo, 2002).

The pre-classification approach, i.e., image-to-image comparison or spectrally-based techniques, involves directly subtracting the land conversion information from two images. It can be further divided into different methods, such as composite analysis (CA), image differencing, principal component analysis (PCA), change vector and spectral mixture analysis (SMA) (Lunetta 1999). CA was described as spectral-temporal change

classification (STCC) technique by Weismiller et al. (1977), which is based upon a single analysis of a multidate data set using standard pattern recognition and spectral classification techniques to identify land cover change areas. PCA is a powerful data transformation technique for information extraction in remote sensing for the analysis of multispectral or multidimensional data (Lillesand et al., 2004). Change vector and spectral mixture (SMA) approaches are more suitable for high temporal resolution data (such as AVHRR) and high spectral resolution (HSR) data analysis, respectively (Lambin and Strahler, 1994a; Gillespie et al., 1990). Image differencing is performed by first applying data transformation to reduce data dimensionality, and secondly, calculating the subtraction results followed by the application of a threshold to distinguish significant spectral differences as areas of land cover change. The thresholds are typically set based on a standard deviation value; the lower the standard deviation, the greater the inclusion and potential for errors of commission (Lunetta, 1999). Optimally, thresholds should be based on the accuracy of categorizing pixels as change or no-change (Fung and LeDrew, 1988). In this method, the data transformation is considered as the most fundamental and widely used approach to accentuate spectral change, hence land cover change (Nelson, 1983). The most important of data transformation methods include: (1) Band ratioing which is used to reduce the data dimensionality associated with multispectral data (Howarth and Wickware, 1981); (2) Normalized Difference Vegetation Index (NDVI) which is the most widely used for all vegetation indices as it only requires red and near-infrared portions of the data (Lunetta, 1999); (3) The tasseled-cap technique that can enhance data interpretability by emphasizing the structures in the spectral data which are related to vegetation, but it is sensor dependent (Crist, 1985). These methods are

generally accurate, but they cannot provide detailed information on how various LULC categories change.

2.1.2 Land Cover and Land Use Classification Methods

Human and natural forces modify the landscape and environment, therefore, resulting in an increased requirement to monitor and assess these alterations. Changes in urban areas affect the corresponding infrastructure supply, energy consumption redistribution, surplus utilizable space, investing conditions, aesthetic and historical values and ambient air quality. These changes, in turn, influence urban planning, environmental management and policy decisions. Information obtained from remotely sensed data on urban land-cover characteristics and their changes over time may be related to ecological, demographic, socio-economic and dynamic aspects of developed regions at various spatial and temporal scales (Phinn et al., 2002).

The study of urban change detection relies mostly on the classification of remote sensing imagery. The various natural and man-made features are identified and categorized in terms of classified LULC maps (resultant images). Most LULC classes follow some classification system. One commonly used is that developed by James Anderson and his colleagues at the U.S. Geological Survey (Anderson et al., 1976). This hierarchical system has four levels. For example, Urban in Level I is broken down in Level II to Residential, Industrial, etc., and then the Residential can be further subdivided under Level III to the units of Single-Family; Multi-Family; Mobile Homes; Hotels/Motels; and

Other. Generally, the higher the Level, the finer the breakdown of the categories will be (RST, 2004). Level I corresponds to coarse spatial resolution data which is categorized to the initial stage application of analyzing rural areas, regional urban systems and exploratory investigation of some of the larger cities in North America (Forster, 1980; Jackson et al., 1980; Jensen, 1981; 1983). Level II relates to medium spatial resolution of 10-30 m data obtained by second generation satellites. It enables the user to identify and map the older, more compact urban characteristics, like Europe with a relatively good accuracy (Welch, 1982; Forster, 1983; Gomarasca et al., 1993; Green et al., 1994). High-resolution satellite imagery, such as IKONOS and QuickBird, can pick up many of the Level III units, whereas, higher resolution is needed for Levels IV.

Conventional Classification Techniques

The classification methods involve two basic modes: supervised and unsupervised. In supervised classification, classes are pre-established according to some prior calibration or training procedure based on a limited number of relatively scarce and costly ground samples. Their efficiency and unbiasedness are largely based on the completeness of training sample coverage, as well as the discrimination (separability) of extracting patterns. Since these requirements are almost impossible to satisfy for a priori ground sampling, the reverse method of unsupervised classification has gained attention (Mokken, 1995).

In unsupervised classification, classes are examined and automatically extracted by classifiers based on the natural groupings or clusters present in the image values

(Lillesand et al., 2004). Clustering algorithms can create clusters in the spectral space of any given number. Afterwards interpretation has to be done manually to assign the proper meaning to corresponding class.

It is well-known that the traditional algorithms for classification of multispectral satellite imagery are per-pixel classifiers which make decision based solely on the spectral information, such as clustering, parallelepiped, minimum distance, ISODATA, maximum likelihood and Bayesian (Jensen, 1996; Campbell, 2002), etc. Conventional practice, with both supervised and unsupervised classification methods, has been mainly based on classical statistical methods and decision theory. Supervised classification relies on linear discriminate analysis, using standard distributional assumptions (normal distribution), Bayesian *a posteriori* allocation and standard maximum likelihood methods. Unsupervised classification can be based on various methods of cluster analysis with similar assumptions (Mokken, 1995). Consequently, these assumptions limit the application of the classification of high resolution multispectral images in urban area. In order to improve the detail and accuracy of per-pixel classification, many reports and papers have been published.

Current Classification Methods

Recent developments in the delimitation of LULC types have focused on procedures for improving the classification process through different ways.

Texture-based methods have been done to determine how groups of neighboring pixels can reveal inherent textural (Webster et al., 1991; Gluch, 2002), contextual (Harris, 1985; Møller-Jensen, 1990), and spatial (Barnsley et al., 1993) properties and patterns.

Neural network analysis methods pertain to examinations based on the neural-net technique. This technique processes both spectral signatures and textural features based on grey-level histograms, such as using artificial neural networks (Civco, 1993; Augusteijin et al., 1995; Foody, 1996), optimized neural nets (Dreyer, 1993), and dynamic learning neural network (Chen et al., 1995), etc.

Fuzzy set-based approaches are used to investigate the composition of the discrete pixels and resolve mixed pixel problems encountered in the classification process. For example, Forster (1985) assumed linear relationships between pixel values and land cover proportions; Fisher et al. (1990) and Wang (1990) adopted fuzzy membership approach; while Shackelford and Davis (2003) suggested a hierarchical fuzzy classification, which develops a "length-width" spatial context measure to make up for the inadequacy of texture measure.

Accuracy issue is another research focus of image classification. Gong and Howarth, (1990) adopted structural information to overcome the accuracy insufficiencies (). Mesev et al. (2001) suggested modified maximum-likelihood classification algorithms to improve the accuracy of conversional maximum likelihood method by linking ancillary spatial data to identify and update the priori probabilities of the maximum likelihood

algorithm. Pedroni (2003) applied an analogical method of modified a prior probabilities to improve classification of Landsat TM data in large and complex landscapes with spectrally mixed land-cover categories. His results showed that the overall classification consistency of the training sites improved from 74.6% to 91.9%, while the overall classification accuracy of sites controlled in the field by independent studies improved from 68.7% to 89.0%.

The joining of remote sensing data coverage with other ancillary spatial data types is defined as the process of geospatial "data integration", and has justifiably received widespread and extensive attention in recent literature (Donnay et al., 2001). With the appearance of advanced GIS software, the integration of remote sensing and GIS has been widely applied and been recognized as a powerful and effective tool in detecting urban LULC changes (Nellis et al., 1990; Pathan, 1993; Jensen and Cowen, 1994; Harris and Ventura, 1995; Liu et al., 2002). According to Wilkinson (1996), satellite remote sensing can be used as a tool to gather data for use in GIS. Thus, GIS data sets can be used as ancillary information to improve the products derived from remote sensing. Remote sensing data and GIS data can be integrated for modeling and analysis. The applications of integrated remote sensing and GIS methods have spread to different aspects of environment monitoring, decision-making and socio-economic management (Landford et al., 1991; 1994; Weng, 2001), etc.

Different spatial and spectral data merging (also called fusion or pansharpening) is becoming a widely used procedure because of the complementary nature of various data

sets (Welch and Ehlers, 1987; Chavez et al., 1991; Zhang, 1999; Gluch, 2002). This fusion is to retain multispectral information together with improved spatial resolution. In addition, it delivers an accurate description of the size, shape and spatial structure of the principal objects/entities found in the city (Ranchin et al., 2001). Therefore, this advances and benefits the higher level and more detailed urban morphologic studies. For example, 10m SPOT Pan data complements 30m Landsat TM data, or 15m Landsat ETM+ Pan data merges with its 30 m multispectral data, and 1m IKONOS Pan data with 10 m SPOT 5 multispectral data. Merging information from different imaging sensors involves two distinct steps (Chavez and Bowell, 1988). First, the digital images from both sensors are geometrically registered to one another. Next, the information contents of spatial and spectral- regions are mixed to generate a single data set that contains the best of both sets (Chavez et al., 1991). Ranchin et al. (2001) developed a new method of sensor fusion, known as ARSIS (Amelioration de la Résolution Spatiale par Injection de Structures). It 'improves' the spatial resolution up to the best available in the combined data set, while still preserving the spectral content of original multispectral images through employing wavelet transformation and multi-resolution analysis to decompose the two images to be merged.

Other processing techniques are continually being explored and documented. Examples of these are: using regression tree algorithm to detect sub-pixel imperviousness change (Yang et al,. 2003), using sampling-based monitoring protocol to detect trend in landscape pattern metrics over a long-term period (Griffith et al., 2003), using a syntactical approach to develop a rule-based system for pattern recognition (Onsi, 2003)

and using ongoing learning techniques to modify the supervised classification method (Barandela and Juarez, 2002). Herold et al. (2003) used the "object-oriented" method to classify and map detailed urban land-use characteristics described by spatial metrics and image texture, while Benediktsson et al. (2003) classified and extracted urban features by means of morphological and neural approaches, etc.

2.2 V-I-S Model Technique

Ridd (1995) suggested a new conceptual model of vegetation–impervious-soil (V-I-S) to enrich urban ecological investigations through remote sensing technology. This model sums up heterogeneous urban areas into simply combinations of basic ground components of V-I-S. It provides an objective and quantitative means of measuring and mapping environmental change caused by urbanization. The objective of this model is to identify and characterize variable land cover patterns to serve ecological/biophysical science purposes (Ridd, 1995).

The model can be explained by a V-I-S diagram (see Figure 2.1). This diagram is a triangle with three axes named V, I and S-axis. Each axis represents one component. Values along the axis are indicated by the percentage of that corresponding component. For example, the different-density residential areas will align with V-I axis, while traditional commercial and industrial areas lie near the I-S axis. Modern industrial and research parks typically pull to the left, depending on the amount of vegetation present (Ridd, 1995).

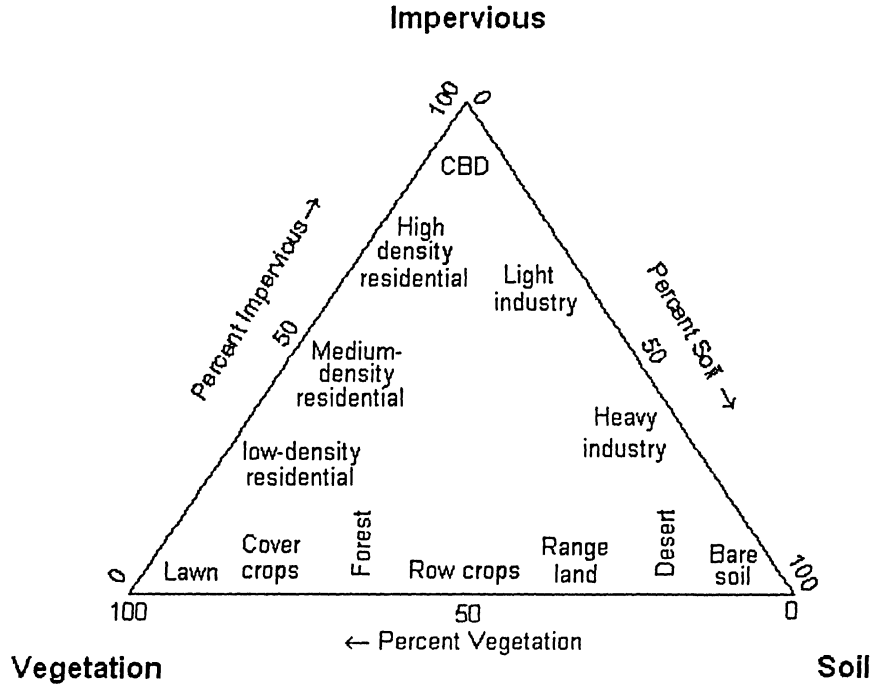

Figure 2.1 Concept of the V-I-S model diagram (Ridd, 1995)

Madhavan et al. (2001), Hung (2001) and Phinn et al. (2002) further verified the effectiveness and usefulness of V-I-S model. The information on V-I-S composition of urban environments is delivered by application of V-I-S model with appropriate image processing methodology. Their results concluded that V-I-S model was an effective solution for studying urban morphology.

2.3 Population Growth Prediction

The quality of human life and the state of the natural and physical environment are inextricably linked in the densely populated urban areas. Often the city developments are well-planned at the microscale (individual buildings and precincts), but the urban

developments are not well-planned at the macroscale. This results in an expanding outward growth (sprawl) driven by the population concentration and successive phase of randomized in-filling of green spaces (Gamba et al., 2003). For this reason, accurate and current population information is of great interest in growing urban and suburban areas for such diverse purposes, such as urban planning, resource management, marketing analysis, service allocation, etc.(Qiu et al., 2003).

Generally, a census is carried out every five to ten years in different countries due to its labor-intensive, time-consuming and costly aspects. More and more attention is drawn to conduct population prediction research using a variety of data and different methods. However, the implementation of these approaches is often complex and expensive due to the requirement of collecting multiple inputs and the involvement of significant manpower (Qiu et al., 2003). The optical satellite data is geared to meeting this challenge. Establishing an easier and cheaper way to solve population estimation is becoming more tractable and is tending to improve with the higher resolution remote sensing data easily available.

The modeling approach often makes use of a new inference process in which the land use categories are related to an urban population variable. The simplest application involves relocating the population figures according to the spatial distribution of residential land which leads to an evaluation of net density figures (Donnay et al., 2001). Although there is still no consensus model or algorithm universally applicable, recent research results are still very encouraging. For example, estimation of population density based on night-time

measurement of visible light patterns (Imhoff et al., 1997; Sutton, 1997), or modeling population density by means of GIS (Langford et al., 1991;1994; Lo, 1995), and alike. Yuan et al. (1997) examined the correlation between population counts from census and land cover types through multivariable regression approach. Pozzi et al. (2002) investigated population density distribution pattern using the relationship between population density and vegetation abundance. Research on population prediction, using single-date satellite imagery, either made use of the extent of residential or urban area measured from image, or directly correlated the pixel brightness values of various bands with population counts (Lo, 2001). Qiu et al. (2003) explored the approaches of using multitemporal satellite images and GIS road data to investigate population growth model at the city level and direct census level. The results showed that accurate population growth estimates were achieved in both methods.

2.4 Chapter Summary

The application of satellite imagery relies heavily on the interpretation and analysis algorithms of digital remotely-sensed imagery. LULC map is one of the most important end-products of imagery interpretation which is obtained from digital image classification process. Urban LULC changes and other socio-economic indicators can be derived on the basis of classified LULC maps. Therefore, the key element of image classification processing is the accuracy and reliability of algorithms to be applied.

Many strategies and techniques have been developed to improve the performance of image interpretation. However, few have found their way into routine use because these techniques can vary greatly in terms of their performance with changes in image characteristics, and in circumstances for targeted studies (Campbell, 2002). Fortunately, several less sophisticated techniques or procedures are quite promising because they have shown experimentally not only to be accurate but also to be comparatively simple and easy to implement in a conventional image processing platform (Yang and Lo, 2002).

Chapter 3

A SATELLITE-BASED APPROACH FOR LAND COVER CHANGE DETECTION AND URBAN POPULATION ESTIMATION

Based on the previous literature review, it has been realized that setting up a simple, applicable and feasible approach to identify urban change and derive corresponding socio-economic indictors is of high importance. This chapter provides a conceptual framework adopted in this study. Section 3.1 gives a concrete description of the study area and data sources. Section 3.2 is the methodology flow chart and detailed explanation. Section 3.3 presents image preprocessing technique and data integration method. Section 3.4 is the summary of this chapter.

3.1 Study Area and Data Sets

3.1.1 Study Area

The study is undertaken in the City of Mississauga, Ontario, one of the fastest growing cities in Canada. It is situated in Peel Region of the Greater Toronto Area (GTA), neighboring the City of Toronto, facing Lake Ontario (Figure 3.1). It covers a total of 336.8 km^2 in area (Industry Canada, 2004) with a population of 612,925 (by 2001). Canada's busiest airport, Lester B. Pearson International Airport, is located within its borders.

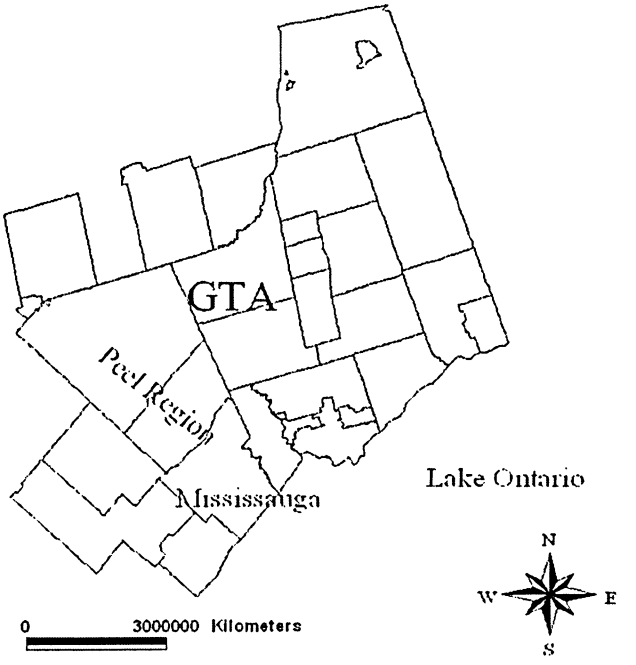

Figure 3.1 Study area -the City of Mississauga in the GTA, Ontario.

3.1.2 Data Sets

Remote Sensing Data

The medium spatial resolution remote sensing data is believed better than the coarse one for urban land cover mapping (Yang and Lo, 2003). Thus, three cloud-free Landsat TM/ETM+ images covering the City of Mississauga are used in this study (see Table 3.1). They are one Landsat-5 TM dataset, obtained on September 20, 1985 and two Landsat-7 ETM+ datasets, acquired on September 3, 1999 and August 10, 2002, respectively. These three Landsat images were acquired in late summer and early fall of August and September. This is the preferred season for LULC analysis, when the land is well covered

by vegetation. These anniversary data sets are selected in order to avoid radiometric differences.

Table 3.1 Selected Landsat TM/ETM+ images used in this study

Sensor	Date	Georeference	Resolution (m)	Bands
Landsat-5 TM	1985-09-20	UTM, 17 zone, GRS 80, NAD83	25	1-7
Landsat-7 ETM+	1999-09-03	UTM, 17 zone, GRS 80, NAD83	30	1- 7 and 8 (Pan)
Landsat-7 ETM+	2002-08-10	None	None	1- 7 and 8 (Pan)

The 2002 image has not been geocoded, while the other two Landsat images have already been rectified and georeferenced to the Universal Transverse Mercator (UTM) map coordinate system, in Zone 17 on the North American Datum of 1983 (NAD83) and GRS 80 ellipsoid. The resolution of 1985 TM image is 25m, while 1999 ETM+ image is 30m. The thermal band of the three Landsat images is not included in the analysis because of their incompatible spatial resolution.

Reference data adopted in this study include 1995 colour digital orthophoto with a resolution of 1m, 1:25,000 hardcopy maps in or close to the year of analysis, GIS-based LULC data, and Mississauga land use planning and designation schedule maps. The reference data are used to validate the classification accuracy and identify city change patterns. It should be noted that the 1995 orthophoto is also used in population growth modelling.

The GIS vector data of administrative boundary of the City of Mississauga and its census-tract boundaries are employed to subset or aggregate the area of interest (AOI).

Population Census Data

The Statistics Canada census data of the City of Mississauga in 1996 and 2001 were used for population growth analysis in this study. The original census data in the City of Mississauga included 119 tracts and 92 tracts in 2001 and 1996, respectively. The tract difference between two years was due to recent developments in the area-of-interest. Fortunately, the population counts which could match the 119 tracts in both years were available.

3. 2 Research Methodology

The objective of this study is to distinguish changes of two land cover features, namely "built-up" and "non-built", and, thereafter, to derive further socio-economic indicators by means of integration with GIS techniques. The methodology scheme adopted in this study is outlined in the following sections.

3.2.1 Change Detection Methodology

The classification-based (map-to-map) method is employed to detect urban land cover changes during the last 20 years using 30m resolution multitemporal Landsat TM/ETM+ data. Figure 3.2 is the flow chart of proposed urban change detection methodology.

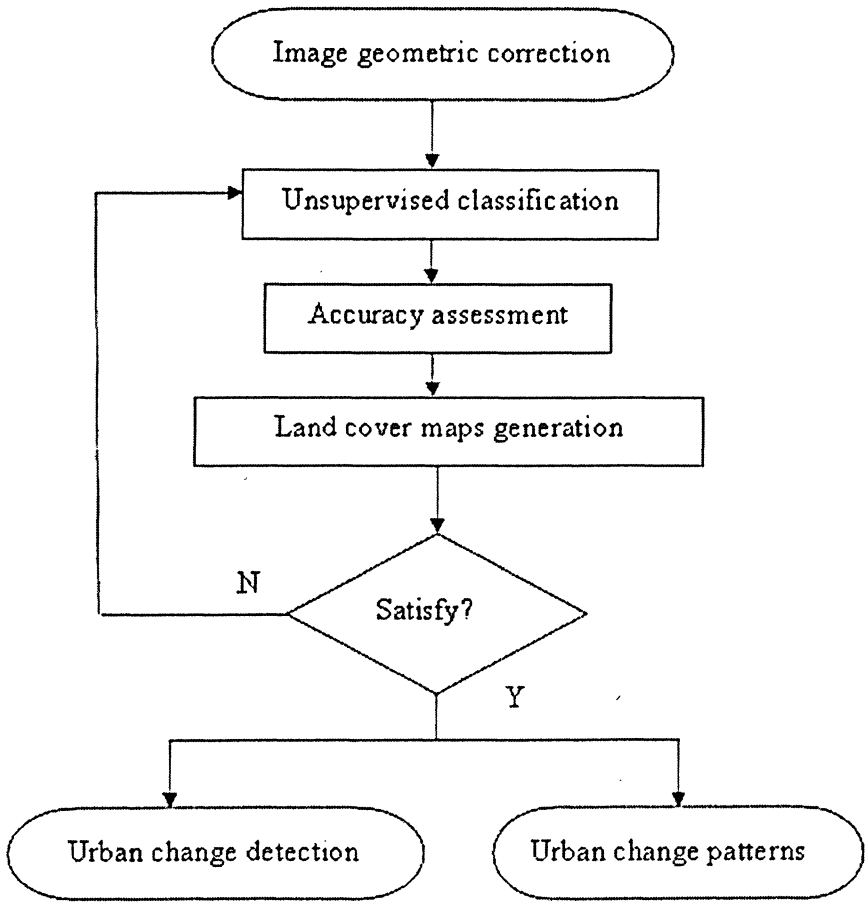

Figure 3.2 Flow chart of urban change detection analysis

First, image-to-image geometric correction is performed to ensure that pixels of each image align in a common map coordinate system. Accurate geometric fidelity is particularly important for change detection analysis. Because analysis is performed on a pixel-by-pixel basis, any misregistration greater than one pixel will provide an anomalous result for that pixel (Lunetta, 1999).

Secondly, in the environment of PC-based ERDAS Imagine V8.7, the multitemporal Landsat TM/ETM+ images are classified by unsupervised approach known as ISODATA

(Iterative Self-Organizing Data Analysis Technique) clustering to generate land cover maps. The ISODAT classifier makes use of the minimum distance method to identify homogeneous spectral clusters iteratively according to the number of clusters specified (Jensen, 1996). The ISODATA technique proves to be the most efficient and accurate approach to identifying spectral clusters of image (Qiu et al., 2003).

Thirdly, the classification accuracy is evaluated in terms of the reference data. The quantity of land cover changes then are derived through a comparison of corresponding classified maps and visually identified via a masking procedure in ERDAS Imagine. The land cover change patterns are recognized by the vegetation-impervious surface-soil (V-I-S) model.

3.2.2 Population Prediction Modeling

Population prediction analysis is accomplished by integrating remote sensing derived data with population census data in a GIS environment. Figure 3.3 depicts the flow chart of proposed methodology.

Since Canada's population census is only carried out every five years, the latest statistic years are 1996 and 2001. In order to use this reliable data resource, exact year-matching images are preferred. If not, the close year images are alternatively employed (Yuan et al., 1997, Qiu et al., 2003).

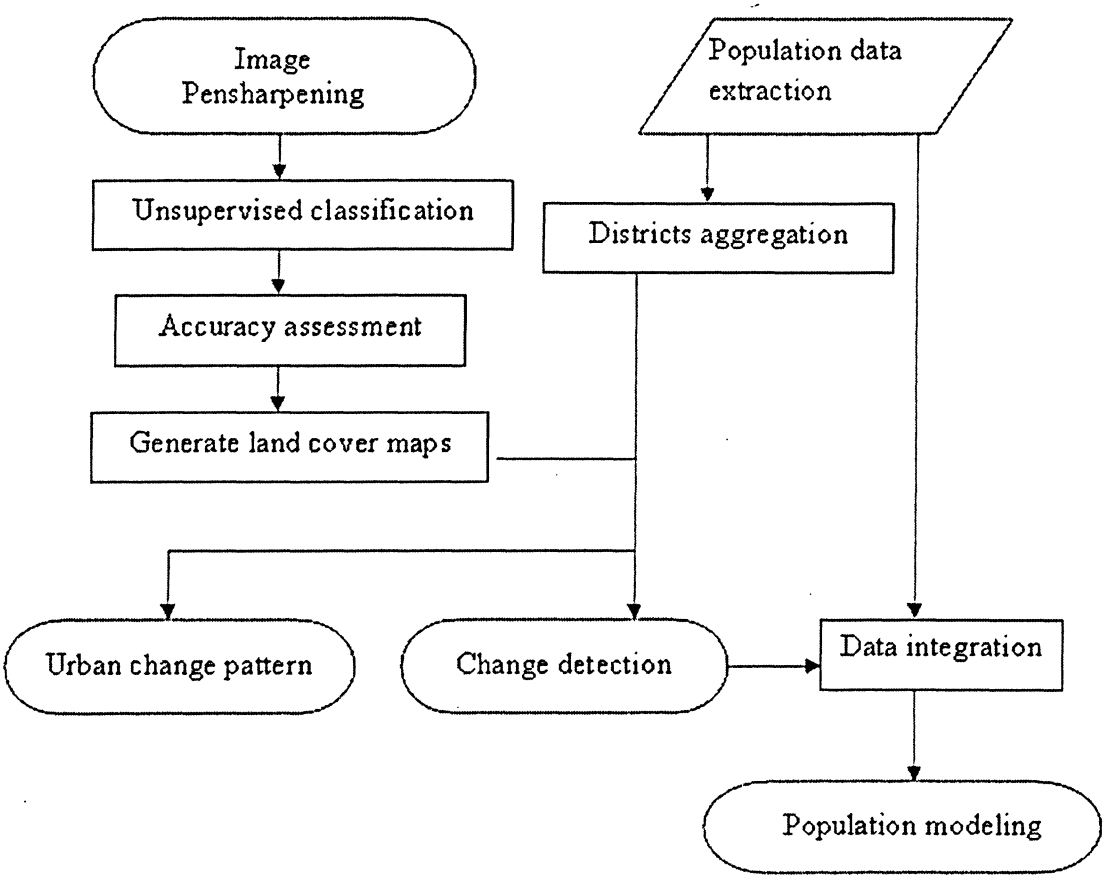

Figure 3.3 Flow chart of population prediction analysis

Hence, in this study, the available images of 2002 Landsat 7 ETM+ and 1995 colour digital orthophoto are selected to support population growth analysis. Due to their mismatch resolutions, the pansharpening technique is employed to obtain 15m resolution Landsat ETM+ data, then 1995 1m orthophoto is georectified and resampled against 15m Landsat ETM+ data to the same map projection and spatial resolution. Land change detection technique, as mentioned in a previous section, is also applied to generate land cover maps. In the mean time, the census tracts are aggregated into city planning districts in a GIS environment. The newly generated district boundaries are used to subdivide classified land cover maps into corresponding areas. The amounts of land cover change

are extracted from each subdivided district. Land cover change patterns are identified according to the actual V-I-S components in each district. An integration of land cover change data with population counts in GIS supports the final population modeling analysis.

3.3 Input Data Preprocessing

3.3.1 Image Geometric Correction

The obtained three images are cloud-free, so no atmospheric correction is required. Because the study area has relatively flat topographic relief, the digital elevation model (DEM) is not employed. However, the 2002 image has no geo-reference information, while the 1985 image has different resolution than the 1999 image. Therefore, image-to-image geometric correction is performed in the ERDAS Imagine 8.7 environment. The road intersections and landmarks are mainly used as ground control points (GCPs) to register, rectify and resample the 1985 and 2002 image against 1999 ETM+ image to the map model of UTM, Zone 17 on the NAD83 horizontal datum and GRS 80 ellipsoid in 30 m resolution using a first-order polynomial transformation and the nearest neighbour resampling algorithm.

The polynomial transformation equation is used to interrelate the geometrically correct (map) coordinates and the distorted-image coordinates. The order is the highest exponent used in the polynomial. A first-order transformation is a linear transformation and is used for relatively even terrain relief. The transformation matrix is computed from the GCPs.

The goal in calculating the coefficients of the transformation matrix is to derive a polynomial equation for which there is the least possible amount of error when they are used to convert the reference coordinates of the GCPs into the source coordinates. (ERDAS Imagine 8.7).

The resampling process is used to determine the pixel values to fill into the output matrix from the original image matrix (Lillesand et al., 2004). The nearest neighbour approach is to assign each "corrected" pixel the value from the nearest "uncorrected" pixel. It has the advantage of simplicity and the ability to preserve original values in the unaltered scene (Campbell, 2002; Lillesand et al., 2004).

In this study, more than the minimum number of GCPs (i.e., GCPs $= \frac{(t+1)*(t+2)}{2}$) for first-order (t=1) polynomial transformation are used. They are dispersed throughout the source and reference image to ensure the accuracy of rectification. Co-registration of the 1985 and 2002 data to the 1999 data are achieved to a root-mean-square (RMS) error of 0.2 and 0.1 pixel, respectively (Table 3.2).

Table 3.2 Rectification of images

Imagery	Spatial resolution (m)	Rectification RMS (pixel)	GCPs	Georeference
1985 Landsat-5 TM	25	0.2	15	yes
1999 Landsat-7 ETM+	30	Reference	Reference	yes
2002 Landsat-7 ETM+	N/A	0.1	17	no

RMS error is the standard measure of the location error. It is the standard deviation of the difference between actual position of GCPs and their calculated positions (i.e., after registration). These differences are known as the residuals (Campbell, 2002).

With 2002 Landsat-7 ETM+ 15m panchromatic band, the 2002 multispectral 30m data is pansharpened into 15m resolution with a map projection of UTM, Zone 17, NAD83 in the PCI Geomatica V9.0 environment. Then 1m colour digital orthophoto of 1995 is coregistered and resampled to the same map projection and spatial resolution of 15m against the 15m pansharpened Landsat-7 ETM+ image. This step is required to ensure these two images are more consistent and suitable for the application analysis. The accuracy of registration is achieved with a RMS error of 0.1 pixel. Since these two images were from different remotely sensed systems, radiometric enhancement step is performed in order to set them in the same analysis base.

The pansharpening refers to the technique that high resolution B&W (panchromatic) imagery is fused with colour (multispectral) imagery to create a high resolution colour image. The spectral characteristics of the original data will be preserved in the resulting high resolution colour imagery. The automatic image fusion algorithm (Zhang, 2002) requires that the Panchromatic channel and the multispectral channels have been co-registered, geocorrected or orthorectified. The best pansharpening results will be obtained if the wavelengths of multispectral bands lie within the spectral frequency range of the panchromatic data (PCI Geomatics, 2004). The discussion of detailed pansharpening algorithm is beyond the scope of this research.

3.3.2 Image Classification

Parameter Setting

The unsupervised classification method adopted in this study is ISODATA (Iterative Self-Organizing Data Analysis Technique) algorithm (Jensen, 1996) which proved to be the most efficient and accurate approach for identifying spectral clusters of the images (Qiu et al., 2003). The parameter setting is predefined as: 10 classes, 15 maximum iterations, and 0.95 convergence threshold. The threshold specifies that as soon as 95% or more of the pixels stay in the same cluster between iterations, the utility should stop processing. This threshold prevents the ISODATA utility from running indefinitely. The classification scheme of 10 classes is based on the study's interest which focuses on the identification of built-up (urban) and non-built land features, or vegetation-impervious surface-soil/open space component to establish V-I-S patterns. To this end, each of the 10 spectral classes is assigned to an appropriate information class in the classified land cover maps and then grouped into one of the required land cover classes, i.e., built-up, non-built and water, or vegetation-impervious surface-soil/open space.

Accuracy Assessment

The validation of classification results is implemented by utilizing the accuracy assessment method in a PC-based ERDAS Imagine 8.7 environment. The "stratified random" function is used to create sample points for all classified images. The generated random points which fall into each land cover category are compared to the reference data. The evaluation results are showed in two kinds of reports: the classification error

matrix (also called confusion matrix) and the accuracy report (See chapter 4). The error matrix simply compares the reference points to the classified points in an $n \times n$ matrix, where n is the number of classes. The accuracy report calculates statistics of the percentages of accuracy, based upon the results of the error matrix. Two important indices, namely overall accuracy and Kappa, are mainly adopted to determine the accuracy of the classification.

The overall accuracy is a percentage of total correctly classified pixels. It is used to indicate the nature of errors of the producer and user (ERDAS, 2003).

The Kappa statistic is a measure of the difference between the actual agreement between reference data and an automated classifier and the change agreement between the reference data and a random classifier. It serves as an indicator of the extent to which the percentage correct values of an error matrix are due to "true" agreement versus "chance" agreement. For example, a value of 0.67 implies that an observed classification is 67 percent better than on results based on chance (Lillesand et al., 2004)

Change Detection and Urban Growth Analysis

The change detection is conducted by comparing different classified land cover maps. The quantity of urban growth is derived from the substraction of the corresponding two land cover maps. Urban change area is visually displayed by masking out existing built-up area in the previous year using mask procedure in the environment of ERDAS Imagine 8.7.

3.3.3 V-I-S Pattern Recognition

For a 17-year land cover change analysis, the City of Mississauga is divided into four different sections according to the administrative map and using existing roads as natural boundaries. The four sections are southeast region, middle part, international airport area and northwest section (Li and Zhao, 2004). In each section, evaluating points are randomly generated using the same method as in accuracy assessment procedure. Their spatial components of V-I-S are compared to reference data. The outcome is tabulated and displayed in a V-I-S triangle diagram.

For population growth modelling, the components of V-I-S are directly derived from subset classified land cover maps in terms of amounts of vegetation, impervious surface and soil/open space.

3.3.4 Population Data Pre-processing

Population Data Aggregation

There were a total of 119 census tracts in the City of Mississauga based on the 2001 data. The census tract (CT) data were in the format of GIS-based polygon shapefile and included relevant spatial attribute information, such as city ID, CMA (Census Metropolitan Area) ID, Province ID, etc., but had no population counts. Therefore the first step is to extract the required population counts from Statistics Canada census data, and then integrate them with corresponding tracts. The second step is to aggregate the

census tract level data into big planning district level data according to their relevant location and adjacent relationship by means of GIS software. This aggregation is to derive new planning district boundaries, as a result, to ensure that the population modeling will be closer to the actual situation and has a more meaningful level of accuracy.

Remote Sensing Data and Population Counts Integration in GIS

The administrative boundary vector datum is used to subset all obtained and georectified images into the City of Mississauga area. This will minimize the computing loads and ensure that the analysis is only performed in the study area of interest. For further population analysis, the newly aggregated planning district boundaries are employed to subdivide the classified land cover maps into the corresponding district areas. The amount of actual land cover change is extracted from the corresponding district. The extracted data, in turn, are used as input data of GIS to integrate with population census data. Based upon the integration data, the population prediction modeling is undertaken using regression analysis approach.

3.4 Chapter Summary

Based on the Chapter 2 literature review and following the objectives of this study, a simple, applicable and feasible solution is set up in this chapter in order to obtain reliable and precise land cover change and corresponding population growth information from optical satellite remotely sensed imagery. The designed methodology includes

unsupervised classification, V-I-S model recognition, pansharpening technique, integration GIS approach and regression analysis. The procedure flow chart and analysis dataset preprocessing are predefined in this chapter.

Chapter 4

LAND COVER CHANGE DETECTION: RESULTS AND ANALYSIS

The designed study framework is implemented in the City of Mississauga. The corresponding results obtained from the analysis are presented in the subsection of this chapter. Section 4.1 introduces the subset of the area of interest. The layout of the classified land cover maps are illustrated in Section 4.2. Accuracy assessment of classification is given in Section 4.3, while urban land cover change detection is depicted in Section 4.4. Section 4.5 describes the V-I-S model recognition results. The summary of this chapter is in Section 4.6.

4.1 Introduction

The subsets of the area of interest for 30m resolution images in false colour are shown in Figure 4.1. Red colour implies vegetation, cyan for impervious surfaces and black for water bodies. From these three false colour images, the urban sprawl of the City of Mississauga can visually be identified over a 17-year period. More remarkable, is the increase of built-up area in the north central and western parts.

Before subdividing the 15m resolution images, an obvious contrast between 30m and 15m pansharpening Landsat-7 ETM+ images and between 1m and 15m degraded digital orthophoto images is given in Figure 4.2.

(a) (b)

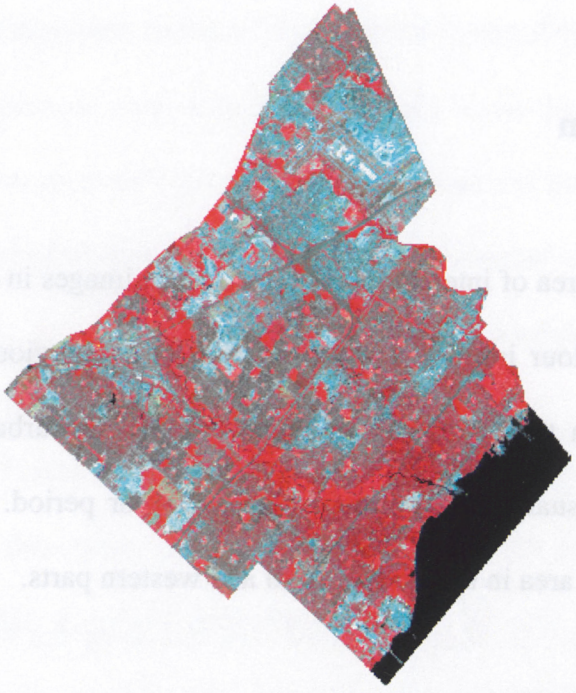

(c)

Figure 4.1 Landsat images covering the City of Mississauga in band 4,3,2: (a) 1985 TM , (b) 1999 ETM+ and (c) 2002 ETM+

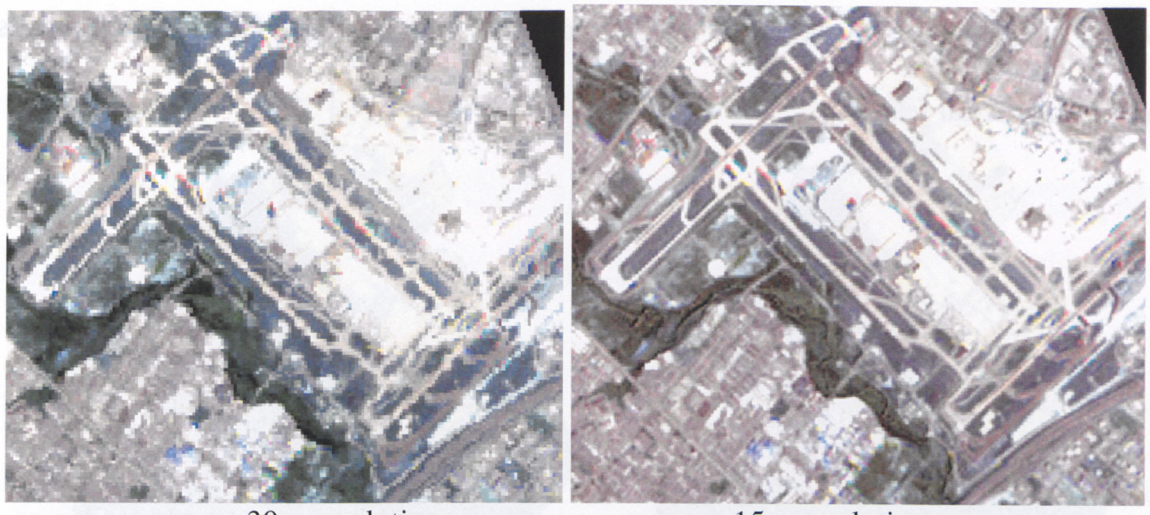

30m resolution 15m resolution

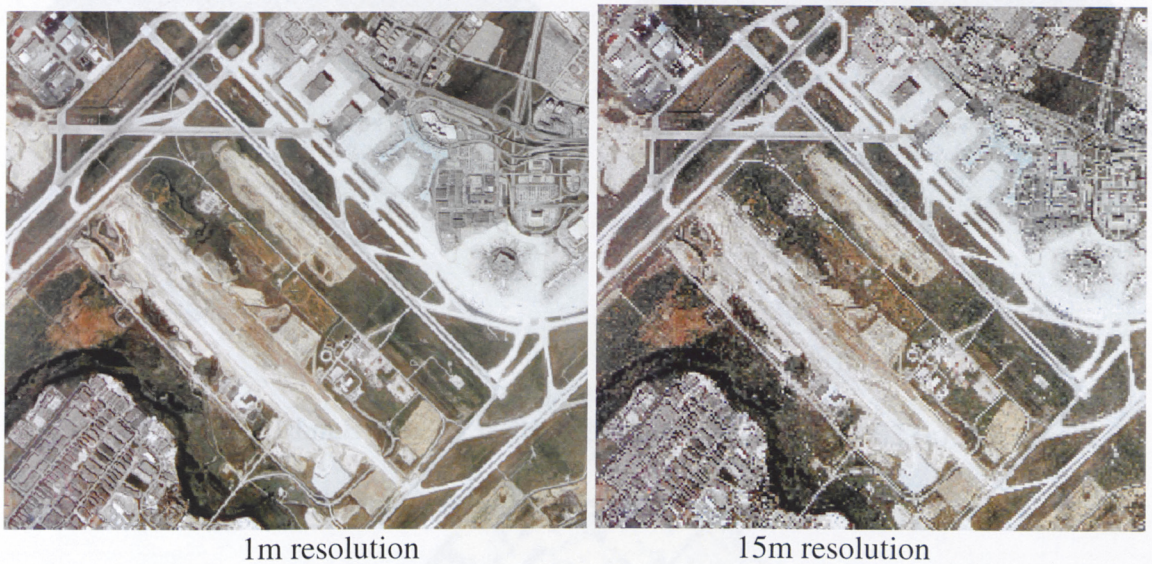

1m resolution 15m resolution

Figure 4.2 Upper: Contrast of 30m and 15m pansharpened Landsat ETM+ image (2002), Below: Contrast of 1m and resampled 15m orthophoto (1995)

The subsets of the 15m 2002 pansharpened image and the 15m resampled colour digital orthophoto in real colour (Bands 1, 2, 3) are presented in Figure 4.3. The water area of Lake Ontario is excluded from the area of interest. Since the 1995 image is only three-band mosaic orthophoto, there is some blur and unbalanced colour difference existing

within the study area in the upper middle part. This will affect the classification results based on spectral feature.

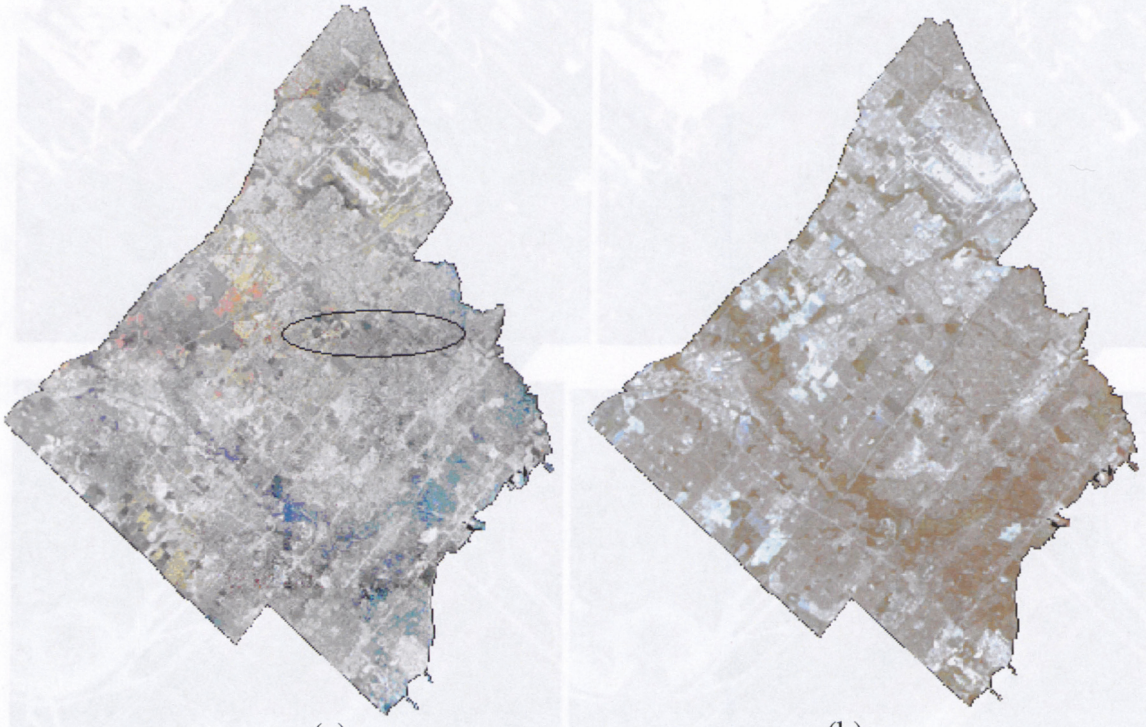

(a) (b)

Figure 4.3 (a) 2002 Pansharpened 15m Landsat ETM+ (Band 1,2,3) and (b) 1995 resampled 15m orthophoto image (Band 1,2,3)

4.2 Unsupervised Classification Results

According to reference data and visual interpretation of spectral or spatial enhanced raw images, 10 classified spectral clusters are assigned to appropriate land cover classes, such as open spaces, golf courses, parks, residential areas, industrial zones, road networks, commercial centers, and alike. These classes are grouped into three composite classes referred to built-up, non-built and water body for long-term urban change analysis, or vegetation, impervious surface and soil for population growth analysis.

(a) (b)

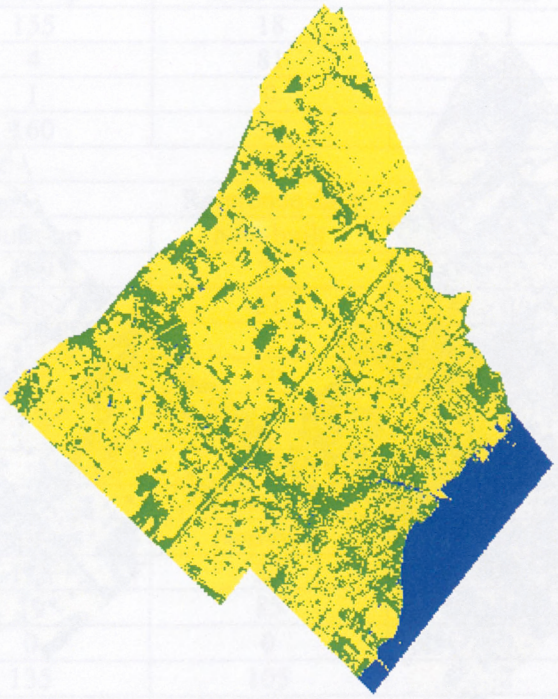

(c)

Figure 4.4 Unsupervised classified land cover maps: (a) 1985, (b) 1999, and (c) 2002 in a spatial resolution of 30m.

Figure 4.4 displays the 30m resolution classified land cover maps. The yellow area represents built-up area, blue for water body and green for non-built area including vegetation, soil, open space, etc. Apparently, the classified land cover maps match quite well with corresponding original Landsat images.

Figure 4.5 represents the 15m resolution classified land cover maps. The yellow and green colours indicate built-up and non-built area, respectively. As previously mentioned, the 15m land cover map of 1995 has an obvious misclassification in the upper middle part due to the unbalanced spectral blur.

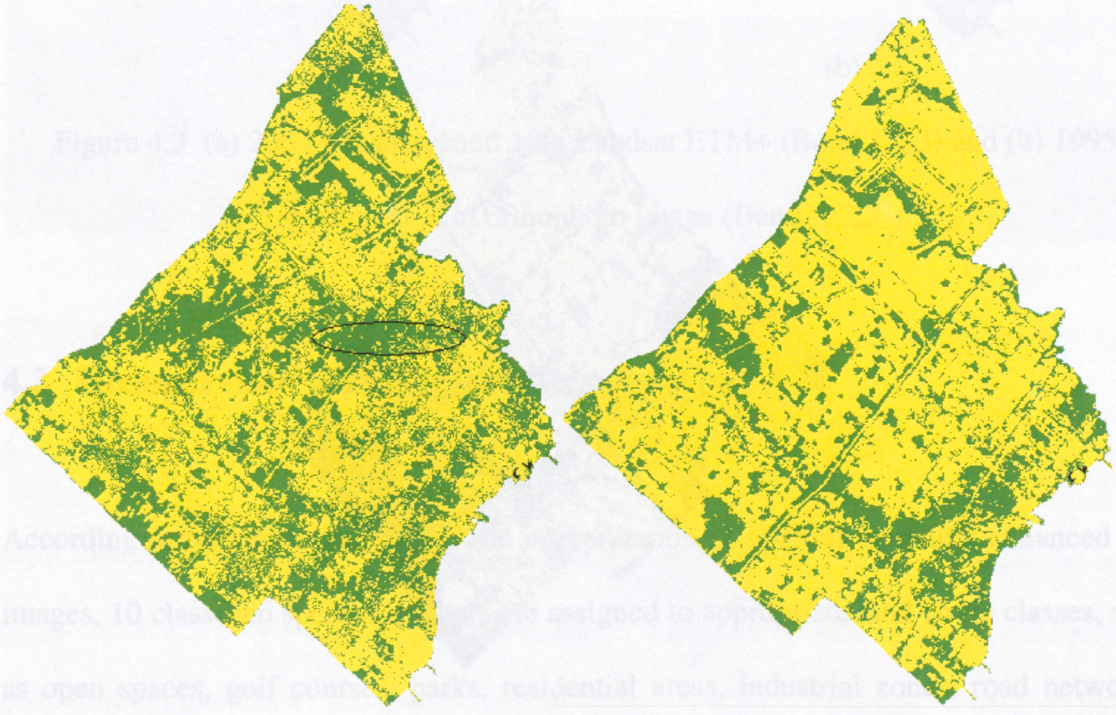

Figure 4.5 15m resolution land cover maps: 1995 (left), 2002 (right)

4.3 Accuracy Assessment Results

The classification accuracy of each image is evaluated using a stratified random sampling design. The results are presented in Tables 4.1, 4.2.

Table 4.1 Error matrix report from classification

For 30m resolution				
1985				
Classified data	Reference data			Row total
	Built-up	Non-built	water	
Built-up	98	10	1	109
Non-built	6	119	0	125
Water	0	0	23	23
Column total	104	129	24	257
1999				
Classified data	Reference data			Row total
	Built-up	Non-built	water	
Built-up	155	18	1	174
Non-built	4	81	0	85
Water	1	0	24	25
Column total	160	99	25	284
2002				
Classified data	Reference data			Row total
	Built-up	Non-built	water	
Built-up	169	9	1	179
Non-built	10	51	0	61
Water	0	0	22	22
Column total	179	60	23	262
For 15m resolution				
1995				
Classified data	Reference data			Row total
	Built-up	Non-built	water	
Built-up	118	20	1	139
Non-built	19	85	1	103
Water	0	0	0	0
Column total	135	105	2	242
2002				
Classified data	Reference data			Row total
	Built-up	Non-built	water	
Built-up	161	9	0	170
Non-built	10	61	1	72
Water	0	0	0	0
Column total	171	70	1	242

Table 4.2 Report of classification accuracy assessment

For 30 m resolution					
1985 classified map: 257 sample points					
Class name	Reference total	Classified total	Number of correct	Producer's accuracy (%)	User's accuracy (%)
Built-up	104	109	98	94.2	89.9
Non-built	129	125	119	92.3	95.2
Water	24	23	23	95.8	100
Column total	257	257	240	Overall accuracy=93.4	Overall Kappa(κ)=0.89
1999 classified map: 284 sample points					
Class name	Reference total	Classified total	Number of correct	Producer's accuracy	User's accuracy
Built-up	160	174	155	96.9	89.1
Non-built	99	85	81	81.8	95.3
Water	25	25	24	96.0	96.0
Column total	284	284	260	Overall accuracy=91.5	Overall Kappa(κ)=0.84
2002 classified map: 262 sample points					
Class name	Reference total	Classified total	Number of correct	Producer's accuracy	User's accuracy
Built-up	179	179	169	94.4	94.4
Non-built	60	61	51	85.0	83.6
Water	23	22	22	95.7	100
Column total	262	262	242	Overall accuracy=92.4	Overall Kappa(κ)=0.84
For 15 m resolution					
1995 classified map: 242 sample points					
Class name	Reference total	Classified total	Number of correct	Producer's accuracy	User's accuracy
Built-up	135	139	118	87.4	84.9
Non-built	105	103	85	81.0	82.5
Water	2	0	0	0	0
Column total	242	242	203	Overall accuracy=83.9	Overall Kappa(κ)=0.67
2002 classified map: 242 sample points					
Class name	Reference total	Classified total	Number of correct	Producer's accuracy	User's accuracy
Built-up	171	170	161	94.2	94.7
Non-built	70	72	61	87.1	84.7
Water	1	0	0	0	0
Column total	242	242	222	Overall accuracy=91.7	Overall Kappa(κ)=0.80

The producer's accuracy indicates how well training set pixels of the given cover type are classified. The user's accuracy is a measure of commission (inclusion) error and indicates the probability that a pixel classified into a given category actually represents that category on the ground (Lillesand et al., 2004).

$$\text{Producer's accuracy}=\frac{X_i}{\sum X_{ref}} \tag{4-1}$$

$$\text{User's accuracy}=\frac{X_i}{\sum X_{class}} \tag{4-2}$$

where, X_i is the observation for correctly classified numbers in each class,

$\sum X_{ref}$ is the total observation for reference data in each class,

$\sum X_{class}$ is the total observation for classified data in each class.

$$\text{Kappa (K)} = \frac{N\sum X_{ii} - \sum X_{class} * X_{ref}}{N^2 - \sum X_{class} * X_{ref}} \tag{4-3}$$

Here, Kappa calculation is based on Table 4.1 error matrix, and

N is the total number of observations,

X_{ii} is the observation for correctly classified numbers,

X_{class} is the observations for classified data,

X_{ref} is the observation for reference data.

For the 17-year land cover change analysis, the accuracy of the classified results is evaluated in terms of 30m resolution Landsat multispectral images. An overall classification accuracy of over 91% and a Kappa coefficient of exceeded 0.84 are

achieved for three-date images, and the accuracy of the 1985 Landsat-5 TM image is a little higher than the 1999 and 2002 Landsat-7 ETM+ images. This confirms the research result in the past that the enhanced spectral sensor brightened the details of urban features; therefore, created more challenges for distinguishing salt-and-pepper effects in complex urban environments (Yang and Lo, 2002).

For population modeling, the accuracy of classified results is validated based on 15m resolution images. The overall accuracy and Kappa for the classified 1995 digital orthophoto are 83.9% and 0.67, respectively, and for the 2002 Landsat-7 ETM+ pansharpened image, the overall accuracy and Kappa are 91.7% and 0.80.

It is evident that the pansharpened 2002 15m Landsat-7 ETM+ image does not help to improve the accuracy of image classification and has only similar or even lower accuracy than 30m images. This scenario has been revealed by previous research, i.e., the improved spatial resolution can lead to an increase not only in the inter-class variability but also in the intra-class variability, which can produce poor image classification accuracy if a classic per-pixel classification method is used (Markham and Townshend, 1981; Williams et al., 1984; Irons et al., 1985; Haack et al., 1987).

The 1995 orthophoto has a lower accuracy of classification than Landsat images. This is because 1m aerial orthophoto is a mosaic of different subset images that may be taken at a different time period. When degraded to 15m spatial resolution, the orthophoto loses a lot of subtle information and generates more mixed pixels, which causes the accuracy to

decline. Another reason worth noting is that the aerial orthophoto has only three bands of spectral reflection which gives less information than six bands.

The detailed error matrix report (see Table 4.1) shows that all the points classified as water are almost always water pixels, the accuracy ranges between 96.0% and 100%. There are 6.0 to 8.0% of the points which are misclassified between built-up and non-built pixels for all 30 m resolution images.

Since Lake Ontario is excluded from the subsets of the 15m images, the remaining small watercourse areas are not easily extracted by the software as a cluster according to their spectral mean and deviation. Hence, the water pixels are not classified, but rather identified by referenced data. The 2002 classified image has only about 8.0% misclassification between built-up and non-built pixels, while 1995 classified aerial orthophoto has almost a 17% misclassification error. These errors are reasonable considering that the degraded 1m aerial orthophoto has only three spectral bands. The errors found in the classified orthophoto need to be adjusted in order to perform further analysis.

4.4 Urban Change Analysis

In addition to computer a classification confusion matrix, classified land cover maps also provide information of the area for each land cover category. Accordingly, the urban change analysis can be carried out by comparing each of the two land cover maps.

4.4.1 Urban Growth over a 17-Year Interval

The areas of each land cover type are statistically extracted from corresponding land cover maps. The substantial growth of built-up area is visually displayed in Figure 4.6 with masking procedure, in which blue is the water area, white is the mask of exiting built-up area in the previous year scene and red is the new built-up area in the after year scene. The amounts of new built-up areas are quantitatively exhibited in Table 4.3 by subtracting corresponding land cover categories.

It is very clear that the greatest changes occurred in the western and north central regions of the City of Mississauga from 1985 to 2002. These are the areas which supply most of the utilizable space and therefore promote the main new development area at the expense of largely losing forest and cropland area. The development of transportation facilities within the study timeframe, such as highways (e.g., Highways 401 and 403) and the Pearson International Airport, has induced an excellent investment environment and further triggered fast construction of residential areas and industrial zones. This will be confirmed by following urban change pattern recognition.

It is also worth mentioning that some errors would cancel each other while overlaying two classified maps. For example, old low-residential areas are misclassified as non-built areas, bare soil as a construction beginning stage and such. This is true because the same salt-and-pepper effect (mixed pixels) in classification procedure appears in each of the raw images.

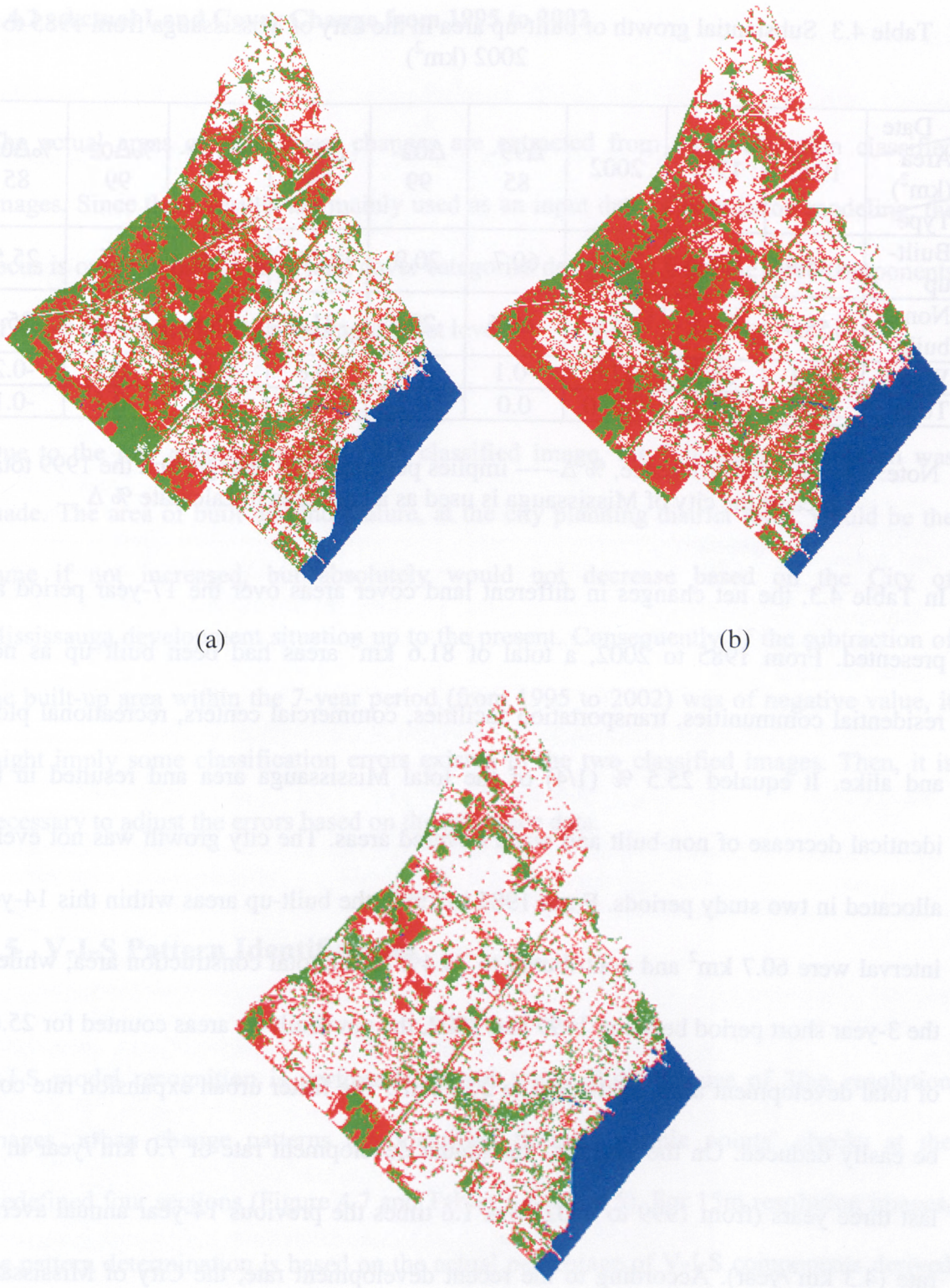

(a) (b)

(c)

Figure 4.6 Urban change results by masking procedure: (a) 1985-1999, (b) 1985-2002 and (c) 1999-2002

Table 4.3 Substantial growth of built-up area in the City of Mississauga from 1985 to 2002 (km^2)

Date / Area (km^2) / Type	1985	1999	2002	Δ99-85	Δ02-99	Δ02-85	%Δ99-85	%Δ02-99	%Δ02-85
Built-up	135.9	196.6	217.5	60.7	20.9	81.6	19.0	6.5	25.5
Non-built	155.9	95.3	74.9	-60.6	-20.4	-81.0	-18.9	-6.4	-25.3
Water	28.4	28.3	27.6	-0.1	-0.7	-0.8	0.0	-0.2	-0.2
Total	320.2	320.2	320.0	0.0	-0.2	-0.2	0.0	-0.1	-0.1

Note: Δ----denotes difference, % Δ----- implies percentage of change, and the 1999 total area of the city of Mississauga is used as a base area to calculate % Δ

In Table 4.3, the net changes in different land cover areas over the 17-year period are presented. From 1985 to 2002, a total of 81.6 km^2 areas had been built up as new residential communities, transportation facilities, commercial centers, recreational plots, and alike. It equaled 25.5 % (1/4) of the total Mississauga area and resulted in the identical decrease of non-built and water covered areas. The city growth was not evenly allocated in two study periods. From 1985 to 1999, the built-up areas within this 14-year interval were 60.7 km^2 and contributed to 74.4% of the total construction area; while in the 3-year short period between 1999 and 2002, the new built-up areas counted for 25.6% of total development area, equivalent to 20.9 km^2. The faster urban expansion rate could be easily deduced. On the average, the annual development rate of 7.0 km^2/year in the last three years (from 1999 to 2002) was 1.6 times the previous 14-year annual average rate (4.3 km^2/year). According to the recent development rate, the City of Mississauga will exhaust its utilizable surplus space in very near future.

4.4.2 Actual Land Cover Change from 1995 to 2002

The actual areas of land cover changes are extracted from 15m resolution classified images. Since these results are mainly used as an input data of population modeling, the focus is only put on the three land cover categories designated from the three components of V-I-S model at the city planning district level.

Due to the low accuracy of the 1995 classified image, the following assumption was made. The area of built-up land feature, at the city planning district level, would be the same if not increased, but absolutely would not decrease based on the City of Mississauga development situation up to the present. Consequently, if the subtraction of the built-up area within the 7-year period (from 1995 to 2002) was of negative value, it might imply some classification errors existed in the two classified images. Then, it is necessary to adjust the errors based on the reference data.

4.5 V-I-S Pattern Identification

V-I-S model recognition is performed in two ways. With the use of 30m resolution images, urban change patterns are identified through sample points' checks at the predefined four sections (Figure 4.7 and Tables 4.4 and 4.5). For 15m resolution images, the pattern determination is based on the actual percentage of V-I-S components derived from 1995 and 2002 land cover map at the planning district level (Figure 4.8).

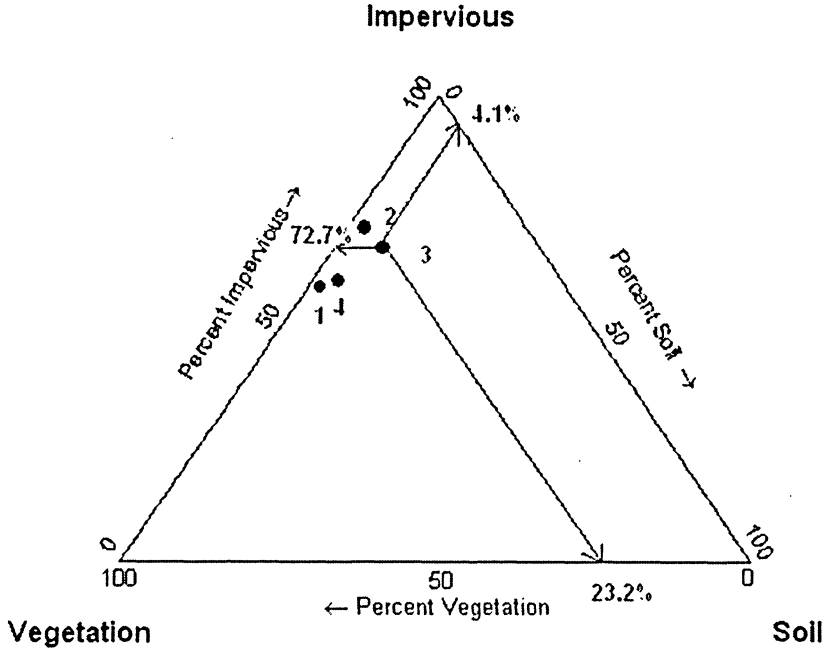

Figure 4.7 Urban change patterns of 2002: 1-mature residential area, 2-city centre, 3-industrial dominance, 4-growing residential area

Table 4.4 Features of four sections of Mississauga in 2002.

Section name	Location	Features
1. Southeast region	South of Dundas Road, include south part of Erin Mill and Cooksville, Port Credit district	mature city region, low-density residential area, concentrated parks and golf course, high-density trees and partial existed industrial zone, face lake Ontario, little utilizable space
2. Middle part	South of Highway 403 and its prolongation, north of Dundas Road, include north part of Erin Mill and Cooksville district	City centre, high-density residential area, commercial centre, schools, parks, little industrial area, limit surplus applicable space
3. International airport area	North of Highway 403 and its prolongation, east of Mavis Road, include Pearson international airport and its vicinity, Malton district	Except parts of residential area in north east corner and south west corner, dominant industrial area and fully developed transportation facilities, partial utilizable space
4. Northwest section	North of Highway 403, west of Mavis Road, include Meadowvale and Streetsville district, north Credit River linger in middle	Expanding residential area and corresponding commercial centre, schools, parks, recreation centre, partial new built industrial area, some utilizable space

Table 4.4 enumerates the main features of each section. The land use characteristics are described based upon the 2002 reference data. Table 4.5 provides the urban change pattern information derived from the composition of V-I-S three elements.

Table 4.5 V-I-S composition of four sections of Mississauga in 1999 and 2002.

Section	1999				2002				Description
	V%	I%	S%	Total Sample Points	V%	I%	S%	Total Sample Points	
1. Southeast region	36.4	62.2	1.4	148	36.7	62.2	1.1	180	Pertain to mature residential area, little conversion
2. Middle part	20.2	78.0	1.8	109	23.4	75.3	1.3	103	City centre: limit conversion
3. International airport area	24.0	72.0	4.1	246	23.2	72.7	4.1	194	Developed and developing industrial area, significant conversion
4. Northwest section	32.9	64.2	2.9	173	32.6	63.8	3.5	141	undergoing residential area, considerable conversion
Mean	28.4	69.1	2.6		29.0	68.5	2.5		

Comparing the V-I-S composition between four sections (Table 4.5), obviously, Section 1, in both years, is actually the old mature city district which features the highest vegetation coverage (>36%), lowest soil exposure (≤1.4%) and least impervious surface (62.2%). These results show that this area maintains its urban morphology of low-density residential area with a relative resistance to commercial expansion.

In contrast, Section 2 reflects a high-density of built-up area (>75%) and a low amount of green space (≤23.5%); 1.8% to 1.3% (from 1999 to 2002) soil exposure depicts that limit

surplus space is undergoing a conversion of land cover and become a focus of new development; the 3% vegetation increase from 20.2% to 23.4% indicates that the city attaches great importance to greenbelt construction.

Section 3 demonstrates a fast pace of development with the highest soil exposure portion (>4.0%). Relatively higher impervious surface (≥72%) and lower green coverage (≤24%) emphasizes that the area is dominated by modern industrial districts. Fully developed transit facilities and systems pledge its further growth and attract more investment.

The features of Section 4 resemble Section 1, but Section 4 has a higher percentage of soil exposure (from 2.9% to 3.5%). It is an expanding residential area with a consideration for future development and environmental protection, by preserving appropriate vegetation, building corresponding commercial centres, schools, parks, recreation centres, communities, and such.

Figure 4.8 illustrates the V-I-S change pattern in 1995 and 2002. The total 31 points represents 31 city planning districts aggregated from population census tracts. Each point has its own V-I-S composition. Remarkable changes can be detected from both land cover maps. In 1995, the 31 points are loosely allocated in the upper middle of the triangle diagram. This implies that these points have less vegetation area but considerable soil/open space which has not been encroached by urban sprawl. They are more likely to belong to urban fringe characteristics and have relatively free space to accommodate further development. However, 7 years later, the 31 points are concentrated to the upper

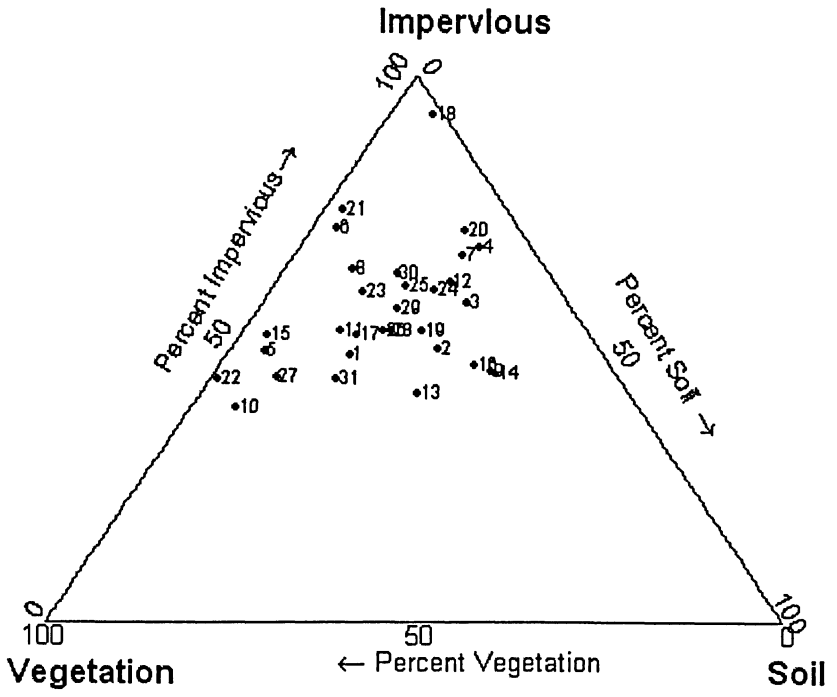

(a)

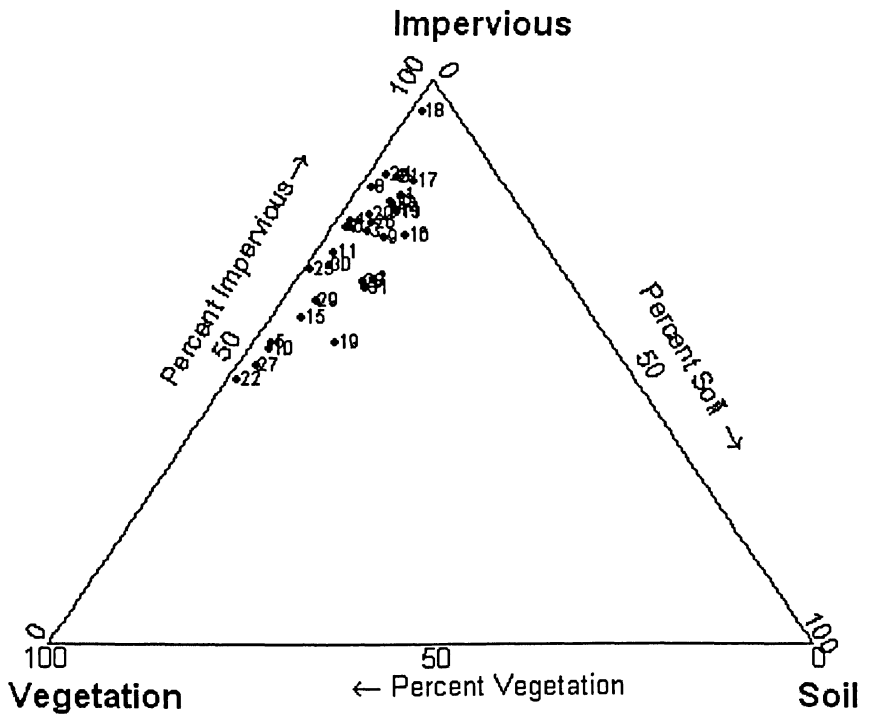

(b)

Figure 4.8 V-I-S patterns at the city planning district level: (a) 1995 and (b) 2002

left corner of the triangle diagram which demonstrates less exposure of soil/open space left and more vegetation area. It comes as no surprise as urbanization is known to take the surplus useful space instead of new construction area.

It is noticed that the modern development ideals have penetrated into the growth of the City of Mississauga which is reflected by its more vegetation coverage instead of soil/open space exposure. In particular, the new built-up industrial areas do not follow the traditional feature which lie near the I-S axis, but pull more to the left along with the V-I axis in the V-I-S diagram. This change creates a beautiful and comfortable working and living ambient, therefore benefits the further development of the city of Mississauga.

4.6 Chapter Summary

Through unsupervised classified land cover, the City of Mississauga's urbanization is clearly revealed in quantitative and visual ways. The total of 81.6 km^2 of built-up areas had erected mainly in the north central part and the western part of the City of Mississauga within 17 year intervals. It equaled 25.5 % (1/4) of the total Mississauga area and resulted in the identical decrease of non-built area and water space. The city's growth rate was not evenly distributed in two periods. According to the annual average development rates, the last 3 years (1999 to 2002) was 7.0 km^2, equivalent to 1.6 times of the previous 14 years' (4.3 km^2).

The urban change can be identified by four distinct patterns in terms of V-I-S components, namely, southeast mature residential area, middle commercial city centre, industrial dominance International airport area and northwest growing residential area.

Chapter 5

URBAN POPULATION ESTIMATE: RESULTS AND DISCUSSION

Based upon the land cover change detection results derived from Chapter 4, the population growth analysis is discussed in this chapter. Section 5.1 describes the census data aggregation results. Section 5.2 discusses the integration of remotely sensed data with population data in a GIS environment. Section 5.3 delineates population prediction modeling and finally, the summary of this chapter is presented in Section 5.4.

5.1 Population Census Data Aggregation Results

According to the Mississauga plan district land use index map, defined by the city planning department of Mississauga, 31 new planning districts are aggregated from 119 census tracts with population counts in ArcView 3.3 platform (see Figure 5.1). It is worth mentioning that the new aggregated planning district boundaries do not exactly match the boundaries of Mississauga plan district land use index map, but follow the census tract boundaries precisely. The 31 new districts' names, with their corresponding population counts, are shown in Table 5.1.

Population growth varied in each district, although total population had increased by 68,543 from 1996 to 2001. Some districts actually had a decrease in population, while others had a significant increase of residents (see Table 5.1). Large population variation

was mostly found in the northwest portion of Mississauga which was categorized as a new residential region and industrial dominant zone. On the other hand, the southeast region of Mississauga, mainly an old residential area with commercial centers and scattered industrial regions, found itself to have some regions with no growth and others with a declining population (see Figure 5.2). It was very interesting to note that the margin of the population counts among the 31 districts reached approximately 45,000 people in both census years.

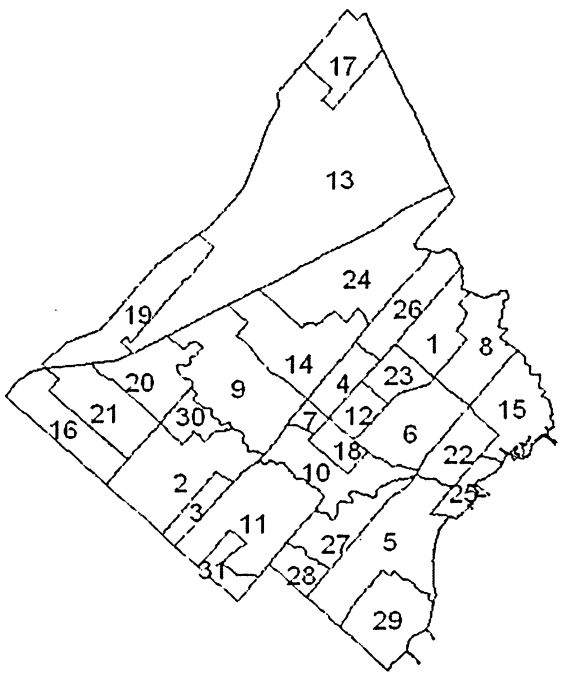

Figure 5.1 Aggregated planning districts

The population difference between 1996 and 2001 varied from minimum disparity of only 15 people to the maximum of 16, 970 people, as a result, there was an average difference of 2,211 people between two years. If this difference was counted as a percentage over the 1996 population base, the amplitude of disparity was stretched between -4.5% and 323.9%. These drastic fluctuations did not necessarily conform to the

area extent of each district or to the basis of population counts in the previous year. This circumstance would lead to population growth modeling on a very variable level.

Table 5.1 Aggregated planning districts with their population counts

Name	number	pop96	pop01	dif_pop0196	%of dif_pop over 96pop
Applewood	1	34,137	34,300	163	0.48
Central Erin Mills	2	17,953	30,530	12,577	70.06
Churchill Industrial Region	3	4,215	4,273	58	1.38
City Centre	4	9,710	9,551	-159	-1.64
Clarkson-Lorne Park	5	33,551	34,321	770	2.30
Cooksville	6	41,379	43,827	2,448	5.92
Creditview	7	5,003	4,872	-131	-2.62
Dixie	8	10,023	10,008	-15	-0.15
East Credit	9	35,237	52,207	16,970	48.16
Erindale	10	21,404	21,196	-208	-0.97
Erin Mills	11	43,614	44,108	494	1.13
Fairview	12	15,143	16,883	1,740	11.49
Gateway+northeast+airport	13	1,303	5,523	4,220	323.87
Hurontario	14	38,477	43,573	5,096	13.24
Lakeview	15	15,951	16,692	741	4.65
Lisgar	16	15,237	24,515	9,278	60.89
Malton	17	38,207	39,715	1,508	3.95
Mavis-Erindale	18	5,576	5,812	236	4.23
Meadowvale Village	19	0	7,685	7,685	N/A
Meadowvale Business Park	20	4,864	4,644	-220	-4.52
Meadowvale	21	41,005	41,811	806	1.97
Mineola	22	9,727	9,665	-62	-0.64
Mississauga Valleys	23	26,544	26,743	199	0.75
Northeast+airport Corporate Centre	24	4,153	8,578	4,425	106.55
Port Credit	25	10,049	9,876	-173	-1.72
Rathwood	26	28,105	27,443	-662	-2.36
Sheridan	27	11,950	12,679	729	6.10
Sheridan Park	28	4,738	4,683	-55	-1.16
SouthDown	29	5,927	5,785	-142	-2.40
Streetsville	30	6,889	7,235	346	5.02
Western Business Park	31	4,311	4,192	-119	-2.76
Total		544,382	612,925	68,543	651.19
Average		17,561	19,772	2,211	21.71
Margin		0 - 43,614	4,192 - 52,207	-662 - 16,970	-4.5%- 323.9%

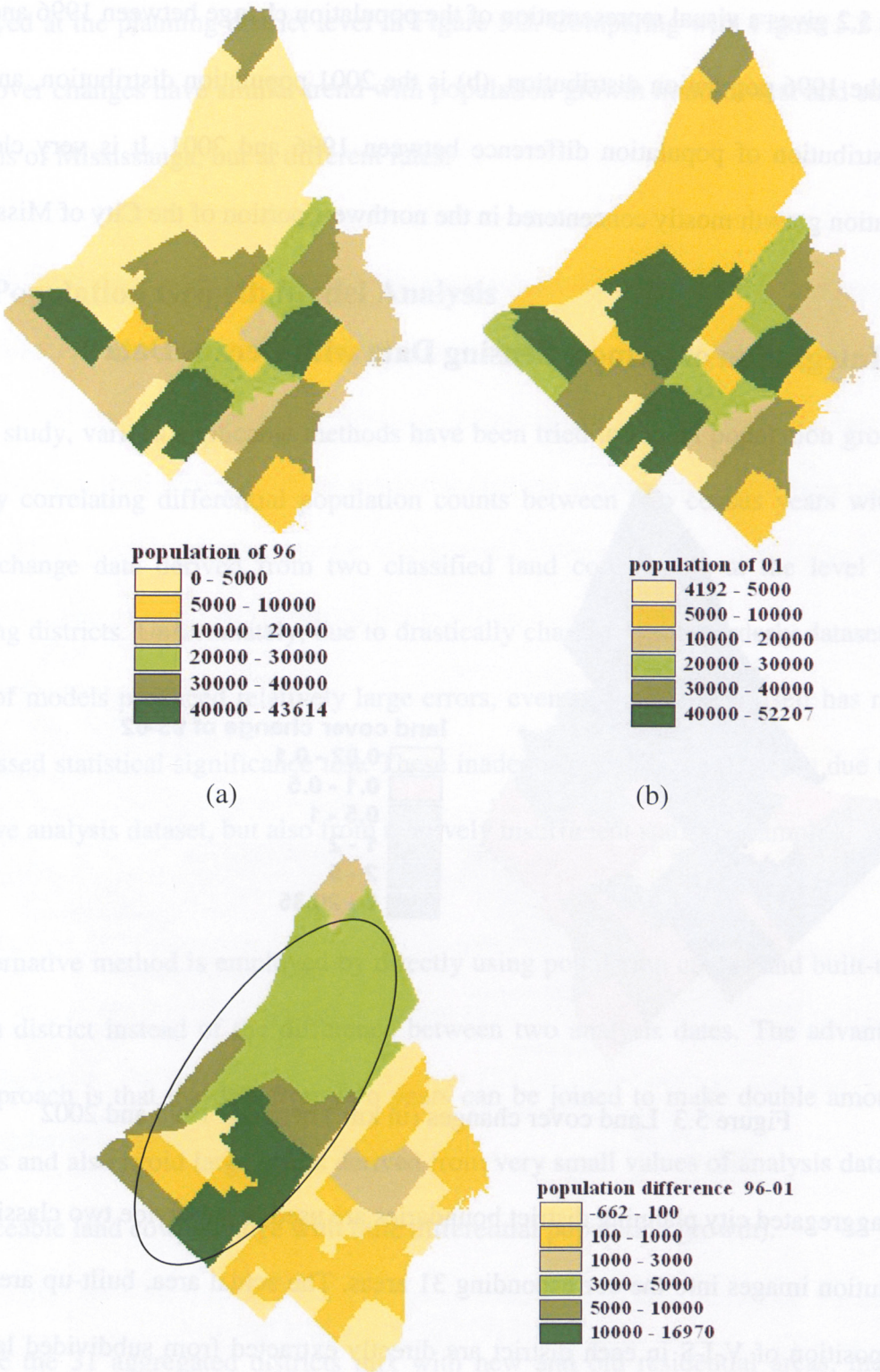

Figure 5.2 Population distribution: (a) 1996 , (b) 2001, (c) the population difference between 1996 and 2001

Figure 5.2 gives a visual representation of the population change between 1996 and 2001, (a) is the 1996 population distribution, (b) is the 2001 population distribution, and (c) is the distribution of population difference between 1996 and 2001. It is very clear that population growth mostly concentered in the northwest portion of the City of Mississauga.

5.2 Integration of Remote Sensing Data with Census Data

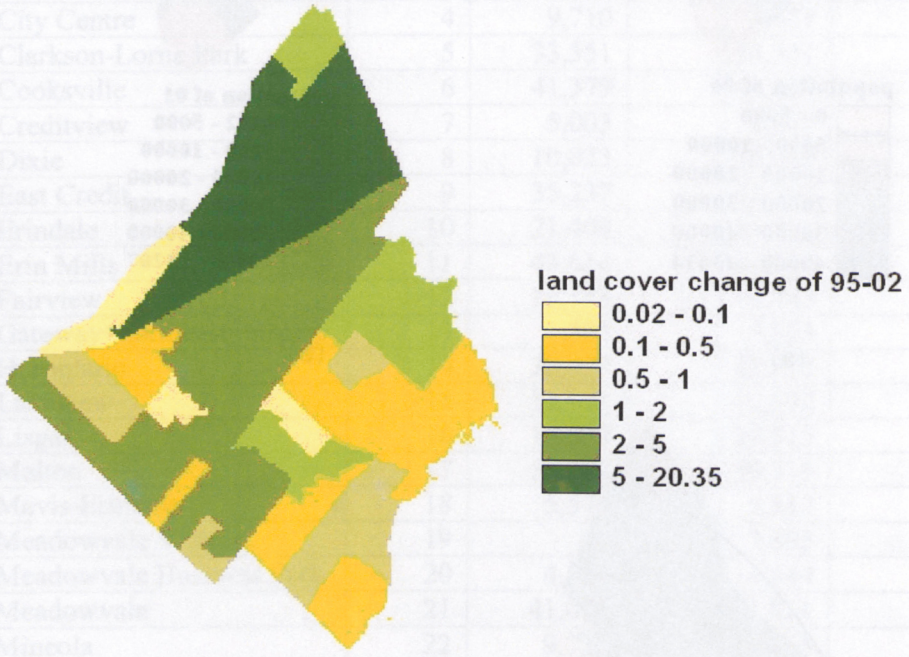

Figure 5.3 Land cover changes (in km^2) between 1995 and 2002

The aggregated city planning district boundaries are used to subdivide two classified 15m resolution images into the corresponding 31 areas. The actual area, built-up area and the composition of V-I-S in each district are directly extracted from subdivided land cover maps. Integration of the land cover change data with population counts is accomplished in the ArcView GIS environment. The land cover changes from 1995 to 2002 are visually

to differentiate between them and to create a clear depiction of the relationship between the population counts and built-up area.

Using 2002 ratio of residential area over built-up area data derived from classified land cover maps, or using GIS-based land use reference data, the typical industrial dominant districts are very clearly pinpointed in both approaches (Figure 5.4).

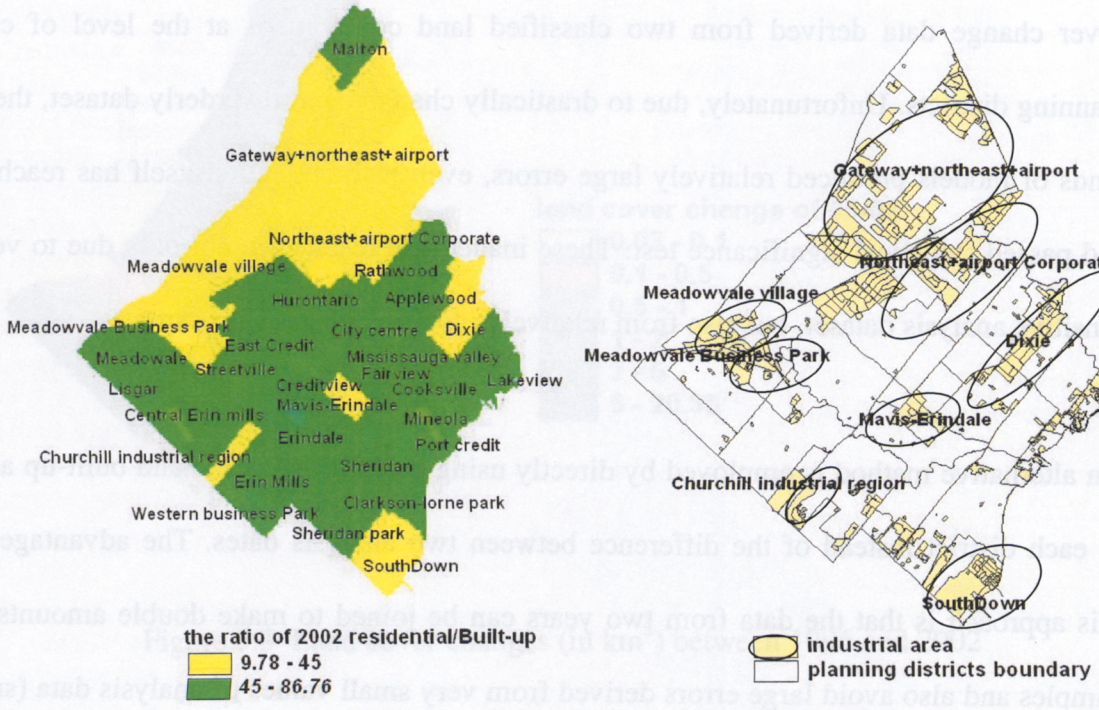

(a) (b)

Figure 5.4 Industrial area identification using (a) 2002 ratio of residential area over built-up area and (b) GIS-based land use data

In Figure 5.4 (a), the ratio value of 45 is chosen as the threshold from the ratio range of 9.8 to 86.8 in terms of distinguishing results comparing with reference land use data.

Since the City of Mississauga is an industrial dominant city, the 45 threshold means that the residential areas in each district only occupy 45% of built-up area, while industrial areas (here means all the non-residential areas) are the remaining 55%. This facilitates the distinction between typical industrial dominant areas, residential dominant areas, and mixed ones. The yellow coloured areas show the typical industrial dominant areas and the green coloured regions are the remaining districts. In Figure 5.4 (b), the yellow indicates the industrial area extracted from GIS-based Mississauga land use shapefile data. From these results, a total of eight typical industrial districts are disaggregated from the grand total of 31. A notable point is that the Meadowvale Village had zero population in 1996, but in 2001, there were 7,685 residents living within its boundaries.

The remaining 23 districts become the candidate samples used in the proceeding analysis. The 1995 and 2002 data are considered as duplicate observations and, thus, are lumped together to get a total of 46 samples. The dependent variable (Y) is the target population counts, while the independent factor (X) in population prediction model is the actual built-up area or the weighted combination area of three elements of V-I-S in each district. For convenience, the two independent variables (X) are called built-up area and "C-442" area, respectively, and they are in area unit of km^2.

The weighted factor for the combination areas of V-I-S components is 4-4-2, which implies that vegetation and impervious surface contribute 40% each, while soil/open space only devotes 20% to the total combination areas of V-I-S. This factor is an empirical value based on the characteristics of the V-I-S model itself and the actual land

cover changes taken place in the city of Mississauga. The purpose of creating this variable is to take into account the land cover of each district as a cohesive whole instead of a single variable of built-up area (impervious surface).

The Pearson correlation coefficient (R) between built-up area or C-442 area and population counts are calculated using all of the 46 samples (Table 5.2). It reveals that there is a significant correlation existing between them.

Table 5.2 Pearson's correlation coefficient between the independent (X) and dependent variable (Y)

Correlation variables	Correlation coefficient (R)	Significance level	Samples
Urban built-up area vs. population counts	0.83	Threshold ρ=0.46 (α= 0.001)	N=46
"C-442" area vs. population counts	0.74		

Out of the total 46 samples, 10 districts are randomly selected and reserved as calibration data for the population prediction models. The remaining 36 samples are used to generate the population prediction model.

The model assumes that the population counts can have a linear or non-linear relationship with the built-up areas or weighted combination area of V-I-S components, and there are no people if there is no built-up area, so the intercept of equation is not necessary.

The tabulated data extracted from integration data of remote sensing and population counts are exported to the MS Excel to perform correlation and regression analysis.

According to the plot graph and statistics ANOVA (**A**nalysis **o**f **Va**riance) results, through trial-and-error analysis, the linear model is adopted for its optimum description of the relationship between population value and built-up area, or "C-442" area. The resultant equations are as follows:

$$PopC=4734.5*B \quad \text{..... (with } R^2=0.92, n=36) \qquad (5\text{-}1)$$

$$PopC=7450.3*C_{442} \quad \text{..... (with } R^2=0.88, n=36) \qquad (5\text{-}2)$$

where PopC is population counts, B denotes urban built-up area in km^2 and C_{442} is "C-442" area of V-I-S in km^2.

From the models shown above, the slope coefficient in the regression equations indicates that every increase of 1 km^2 area in built-up area or in C-442 area is associated with a population growth of around 4,700 or 7,450 people in each district.

The results of ANOVA are given in Table 5.3. It is ascertained that there is a very strong relationship between population counts and built-up area or "C-442" area. This is confirmed with their statistical significance test level which passes with a confidence level of 99.99% (α=0.0001).

These two models are applied to the 10 districts that are withheld to determine the degree of accuracy. The resulting estimates are compared with the actual population counts. The prediction values of the two models have the same change patterns as the actual population counts do. However, some differences exist among them by visual check (see Figure 5.5).

Table 5.3 Regression statistics results

Regression statistics for population and built-up area	
Multiple R	0.96
R Square	0.92
Adjusted R Square	0.89
Standard Error	8158.66
Observations	36

ANOVA

	df	*SS*	*MS*	*F*	*Significance F (α=0.0001)*
Regression	1	2.70E+10	2.70E+10	405.78	1.78E-20
Residual	35	2.33E+09	66563790		
Total	36	2.93E+10			

Regression statistics for population and C- 442	
Multiple R	0.94
R Square	0.88
Adjusted R Square	0.85
Standard Error	10142.62
Observations	36

ANOVA

	df	*SS*	*MS*	*F*	*Significance F (α=0.0001)*
Regression	1	2.57E+10	2.57E+10	250.20	3.04E-17
Residual	35	3.60E+09	1.03E+08		
Total	36	2.93E+10			

An objective examination is required in order to eliminate the visual errors. The various error measures are adopted and presented in Table 5.4. The total percentage error is the ratio of the total prediction error over the total population of 10 validated districts. It is an appropriate indicator of how good the models are as a whole for estimating the overall population. The mean relative percent error is the average of all individual prediction percent error of 10 districts. It is also a good measurement of model performance in individual units, but negative and positive percent errors can cancel each other out.

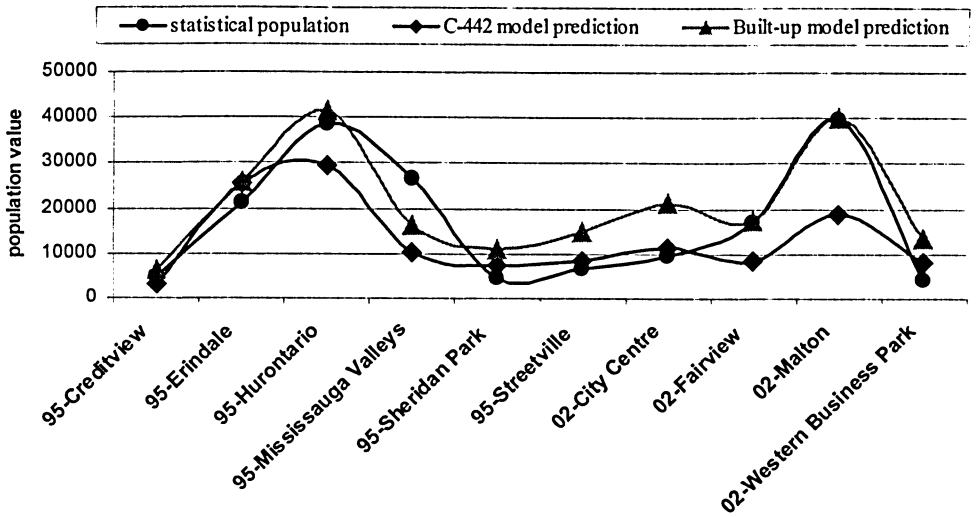

Figure 5.5 Comparison between statistical population counts and population estimation derived from two models

Table 5.4 Error measures for the population prediction models

District	Population counts	Built-up model prediction	Relative % Errors	Population Weighted Abs. % Errors	C-442 model prediction	Relative % Errors	Population Weighted Abs. % Errors
95-Creditview	5003	6233	24.6	0.7	3297	-34.1	1.0
95-Erindale	21404	25899	21.0	2.6	25580	19.5	2.4
95-Hurontario	38477	41594	8.1	1.8	29558	-23.2	5.1
95-Mississauga valleys	26544	16316	-38.5	5.9	10134	-61.8	9.5
95-Sheridan park	4738	10873	129.5	3.5	7364	55.4	1.5
95-Streetville	6889	14876	115.9	4.6	8592	24.7	1.0
02-City centre	9551	21236	122.3	6.7	11239	17.7	1.0
02-Fairview	16883	17452	3.4	0.3	8674	-48.6	4.7
02-Malton	39715	39953	0.6	0.1	18848	-52.5	12.0
02-Western business Park	4192	13421	220.1	5.3	8128	93.9	2.3
Mean	17340	20785	60.7	3.2	13141	-0.9	4.1
Total	173396	207852	19.9	31.7	131413	-24.2	40.5
Mean Abs. % Errors			68.4			43.2	

The mean absolute percent error is a modified and reasonable measure which is derived from the average of absolute individual percent error, but it is often affected by the extremes. Qiu et al. (2003) suggested a new measure and believed it was the best error measure for the individual unit, namely population weighted average absolution percent error. It was defined as the ratio of the population weighted sum of local absolute percent error over the sum of all the populations. This parameter can eliminate the extreme effects on the measure caused by the difference in population (Qiu et al., 2003).

It is clear from Table 5.4 that the built-up area population prediction model gives a positive mean relative error of 60.7% and a mean absolute error of 68.4 %. This is due to the extremely poor overestimated errors (over 100% relative percentage errors) pulling the average errors towards a higher value. These poor estimations occur in the combined districts of residential and industrial or residential and commercial area with relatively lower population. A closer examination reveals that the overall total error and population weighted average absolution error are actually only 19.9 and 31.7, respectively. In other words, the built-up model has reasonable and better prediction power at the level of overall population for all districts and individual population in residential dominant districts with relatively large population counts. On the other hand, the "C-442" model has an opposite and smaller error estimating property compared with the built-up model. Only 0.9% negative average relative error indicates a more stable estimating performance in individual districts, but a 40.5% population weighted average absolution errors reveals relatively larger error for the individual districts. There is no extreme estimation error (over 100% relative percentage errors) occurred, although an overall underestimation

(24.2% negative total percentage errors) is obvious in the C-442 model. Except 2002 Western business park district with the least population has 93.9 % relative errors, in which the industrial area occupies more than half of its total area, the "C-442" area population prediction model demonstrates a narrower prediction fluctuation for non-typical industrial districts.

Figure 5.6 plots the relative percentage errors of population estimation from two models. If ±40% is set up as the threshold to categorize the population prediction value close to its true counts or not, then the accuracy of model prediction is represented.

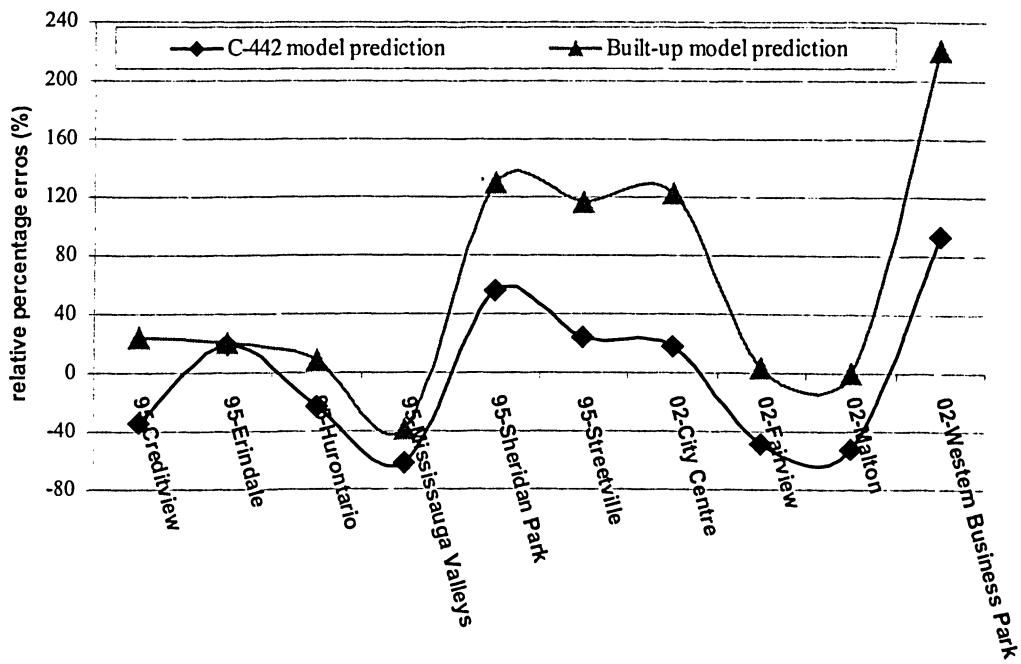

Figure 5.6 The accuracy comparison between two models

Out of the 10 estimates, 6 are very close to the actual population counts in the built-up area prediction model. The remaining 4 predictions have noticeably overestimated values.

One overvalued district is found to be a residential dominant area with lower population counts (1995 Streetville), while the other three are overrated due to their large ratio of industrial and commercial mixture, including 1995 Sheridan Park, 2002 City Centre and 2002 Western Business Park . These errors are entirely induced by the allometric growth of population and land cover changes.

In the "C-442" prediction model, there are 5 out of 10 matches and mismatches with the true population value. Three of them, that are underestimated, are located in typical residential areas with larger population counts; they are 1995 Mississauga valleys, 2002 Fairview and 2002 Malton. The remaining two that are overestimated are the industrial and mixed residential districts, including 1995 Sheridan Park and 2002 Western Business Park.

5.4 Chapter Summary

Initial population census tracts have been aggregated into more meaningful districts according to the city planning district index map of Mississauga. A total of 31 districts have been generated to conduct a population growth analysis. GIS supplies a powerful platform to integrate remote sensing data with the population counts at the city planning district level. Based upon this integration, two population prediction models are established by directly correlating population counts with built-up area or "C-442" area of V-I-S components. The results reveal that a linear equation is the optimum model for the population estimation, and every square kilometer increase in built-up area or in "C-

442" area can be associated with the population growth of around 4,700 or 7,450 people in each district. The evaluation of models shows that the built-up area model is applicable in overall population estimation and individual population prediction in residential dominant districts with relatively large population counts. But this is not true for the industrial or commercial prevalent residential areas. The "C-442" area model has overall stable estimation, but with noticeable underestimation in typical residential area with large population counts.

Chapter 6

CONCLUSIONS AND RECOMMENDATIONS

A simple, reliable and feasible solution is designed in this study in order to provide a quantitative indicator of the fast urban growth that occurred in the past two decades. The multitemporal and multispectral Landsat TM/ETM+ medium resolution images are used to conduct urban change mapping and detection analysis. The 15 m resolution pansharpened Landsat-7 ETM+ image and the resampled colour orthophoto are adopted to explore population growth information derived from fast urbanization. Section 6.1 draws the conclusions of the major achievements and findings. Section 6.2 discusses the limitations found in the results. Section 6.3 outlines some recommendations for further research.

6.1 Conclusions

A satellite-based approach has been set up for the practical application of urban change detection and population prediction modeling. Three dates of Landsat TM/ETM+ images from 1985 to 2002 are employed to map and perceive land cover change of the City of Mississauga. In the past 30 years of urban development, Mississauga has become the sixth largest city of Canada, the third largest city in the province of Ontario and the largest city in the Peel Region in the GTA, Ontario. This dramatic change not only pushes this suburban city towards becoming a modern municipality, but also results in a

decrease of its usable space. The identification and monitoring of the rate of urban change and its pattern plays a very important role in future developments.

Urbanization is described as an alteration of natural surface of an area to man-made-oriented land features. Hence, land cover change is often the attention of urban mapping and change detection.

Land cover maps in this study, primarily focusing on the two major land cover features of built-up and non-built-up areas, are generated using an unsupervised classification method with above 91.0% overall accuracy and exceeded 0.84 Kappa (*k*) index. Urban change rate and its corresponding locations are identified by comparing these classified land cover maps and masking procedure. The results reveal that a total of 81.6 km^2 of net built-up areas occurred within the past 17 years. This is equivalent to 25.5% of the entire Mississauga area. The urban sprawl rates were 7.0 km^2/year between 1985 and 1999, and 4.3 km^2/year between 1999 and 2002. Therefore, a very remarkable contribution occurred in the last three years (1999-2002) of study timeframe which accounted for 74.4% of the total construction area. According to the speed of recent developments, Mississauga could exhaust the remainder of its utilizable space in the very near future.

Changes in urban land cover patterns are recognized by V-I-S model, which help in determining how the city demographic /land cover morphology changes. Four different types of V-I-S combination are identified with the aid of the reference data, namely the southeast mature residential area, middle part of the city center, the north industrial

dominant region and the northwest new residential zone. This pattern recognition has in turn delivered valid information regarding where the construction is undergoing.

Population growth is a vital parameter in the urbanization, not only as a resulting factor, but also as an important driving force. This is why it draws extensive attention in recent studies. Multitemporal remote sensing images are used to investigate population change while conducting the study. In order to take advantage of reliable population data from Statistics Canada census, the 30m 2002 Landsat 7 ETM+ image and 1 m 1995 colour digital aerial orthophoto are adopted. Both images are further processed to the resolution of 15m with the same map projection by pansharpened techniques, geometric corrections and resampling methods.

Population counts at the census tract level are aggregated into larger district levels' according to the framework of city planning district of Mississauga by means of ArcView 3.3. The aggregated 31 districts' boundaries are used to subdivide the 15m resolution classified land cover maps into corresponding 31 parts. The three land cover features of V-I-S components are extracted from subdivided land cover maps. The land cover change patterns in the V-I-S diagram, at the level of planning district, delineates that modern industrial development ideals predominate in the recent growth of Mississauga. More attention to green belt coverage changes the traditional industrial concept of more exposure of bare soil surface. Both population counts and land cover feature information are integrated in GIS environment to conduct population prediction modeling. Two independent variables are adopted, namely actual built-up area and the "C-442" area of

V-I-S. The typical industrial districts are excluded from population modeling due to their allometric relationship between population growth and built-up area sprawl. Trial-and-error methods have revealed that the linear equation is the optimum model to describe the relationship of population counts and the actual built-up area or "C-442" area.

Two population prediction models have been established in terms of actual built-up area and "C-442" area of V-I-S components variable. Both models are evaluated using various error indexes. The results show that the built-up area population model has a better performance in the overall population estimation and individual residential dominant areas with large population counts, but failed in industrial dominated residential areas. The "C-442" area model demonstrates a more stable estimation, but a noticeable underestimation exists in typical residential districts with large population counts.

6.2 Limitations and Discussions

The objective of this study was to first supply a quantitative indication of land cover change and visually represented this alteration patterns occurred in the final twenty years in a fast growing city like Mississauga. Secondly, population prediction modeling was attempted by integrating land cover change information with demographic data at the planning district level in a GIS environment. Unfortunately, the exact year-matching image data were not available, so the analysis could only be accomplished based on the available data sources. The limitations are described as follows:

(1) At the regional level, 30m resolution was sufficient to distinguish straightforward land cover features, but might not deliver detailed land use information at the micro scale with acceptable accuracy.

(2) Unsupervised ISODATA classifier was adopted to implement land cover change detection analysis with a validated classified accuracy. Although it was proved to be the most efficient and accurate approach to identifying spectral clusters of the images, it did not avoid classification errors in the spectral mixed and spectral close pixels.

(3) Because the pensharpened 15m resolution Landsat image did not obviously improve the accuracy of classification using the same classifier as 30m resolution image did, the more applicable method is required in order to take advantage of this higher resolution data.

(4) The 1m colour aerial orthophoto did supply valid reference information to evaluate the classification accuracy, but when degraded to 15m resolution, it introduced bigger classified errors using the same method as Landsat TM images did. These data would, to some extent, affect the analysis accuracy.

(5) Population growth prediction models revealed a lower accuracy if the areas of land cover change between two analysis years were used, not only due to the allometric change of population and built-up area between the years, but also due to the very sensitive population data (i.e., extreme big or small change values).

(6) The established population prediction models based on actual built-up areas and "C-442" areas of V-I-S components need further validation for application using more sample data.

6.3 Recommendations for Future Research

Based on the above discussion, future work can be conducted to refine the analysis results or to overcome the existing limitation found in this study.

Use current techniques or algorithms, like fuzzy, artificial neural network, normalized difference vegetation indices (NDVI) or similar methods to tackle the problem of spectral mixed or spectral close pixels encountered in the image classification processing, thereby improving the classification accuracy.

Use more exact year-matching remotely sensed data to perform more accurate and reliable investigations on population prediction modeling. Eventually, if there are more accurate analysis samples, more statistic circumstances will occur and, thus, a more accurate population estimation will be achieved.

Use more datasets to further examine the reliability and efficiency of established population prediction models.

Employ high-resolution satellite imagery to determine the detailed city morphology change and produce LULC maps in order to timely update physio-geographic input data of GIS.

BIBLIOGRAPHY

Augusteijn, M. F., L. E. Clemens and K. A. Shaw, 1995. Performance Evaluation of Texture Measures for Ground Cover Identification in Satellite Image by means of Neural Network Classifier. *IEEE Transactions on Geoscience and Remote Sensing,* 33(3): 616-626.

Barandela, R. and M. Juarez, 2002. Supervised Classification of Remotely Sensed Data with Ongoing Learning Capability. *International Journal of Geographical Information Systems,* 23(22): 4965-4970.

Barnsley, M.J., S.L. Barr, A. Hamid, J-P. Mullker, G.J. Sadler and J.S. Shepard, 1993. Analytical Tools to Monitor Urban Areas, *Geographical Information Handing: Research and Applications* (P. Mather editor), John Wiley and Sons, Chichester. pp.147-184.

Barnsley, M.J., L. Møller-Jensen and S.L. Barr, 2001. Inferring Urban Land Use by Spatial and Structural Pattern Recognition, *Remote Sensing and Urban Analysis* (J.P. Donnay, M.J. Barnsley and P.A. Longley, editors), Taylor & Francis, London. pp.115-144.

Ben-Dor, E., 2001. Imaging Spectrometry for Urban Application. *Imaging Spectrometry : Basic Principles and Prospective Applications* (Freek D. van der Meer and Steven M. de Jong, editors), Kluwer Academic Publishers, Boston. pp. 243-281.

Benediktsson, J.A., M.Pesaresi and K. Arnasn, 2003. Classification and Feature Extraction for Remote Sensing Image from Urban Areas Based on Morphological Transformations. *IEEE Transactions on Geoscience and Remote Sensing,* 41(9): 1940-1949.

Campbell, J.B., 2002. *Introduction to Remote Sensing, e/3.* The Guilford Press, New York, NY, 620p.

Chavez, P.S., Jr., S.C. Sides and J.A. Anderson, 1991. Comparison of Three Different Methods to Merge Multiresolution and Multispectral Data: Landsat TM and SPOT Panchromatic. *Photogrammetric Engineering and Remote Sensing,* 57(3): 259-303.

Chen, K. S., Y. C. Tzeng, C. F. Chen and W. L. Kao, 1995. Land-cover Classification of Multispectral Imagery Using a Dynamic Learning Neural Network. *Photogrammetric Engineering and Remote Sensing,* 61(4): 403-408.

Civco, D. L., 1993. Artificial Neural Networks for Land-cover Classification and Mapping. *International Journal of Geographical Information Systems,* 7(2): 173-186.

City of Mississauga, 2004. *Mississauga Growth Forecasts- Population Growth,* URL: http://www.city.mississauga.on.ca/PLANBLDG/publications/html/miss_growth_forecast.htm, (last date accessed: 17 February 2004).

Crist, E.P., 1985. A TM Tasseled Cap Equivalent Transformation for Reflectance Factor Data. *Remote Sensing of Environment,* 17 (3): 301-306.

Crisp, 2004. SPOT, France, URL: http://www.crisp.nus.edu.sg/~research/tutorial/spot.htm, (last date accessed: 21 May 2004).

Donnay, J.P., M.J. Barnsley and P.A. Longley, 2001. *Remote Sensing and Urban Analysis*, Taylor & Francis, London, 268p.

Donnay, J.P., M.J. Barnsley and P.A. Longley, 2001. Remote Sensing and Urban Analysis. *Remote Sensing and Urban Analysis.* (J.P. Donnay, M.J. Barnsley and P.A. Longley, editors), Taylor & Francis, London, pp. 1-18.

Donnay, J.P., 1999. Use of Remote Sensing Information in Planning. *Geographical Information and Planning*, (J. Stillwell, S. Geertman and S. Openshaw, editors), Springer-Verlag, Heidelberg, pp. 242-260.

Dreyer, P., 1993. Classification of Land Cover Using Optimized Neural Nets on SPOT Data. *Photogrammetric Engineering and Remote Sensing,* 59(5): 617-621.

Definitions, 2004. Census Metropolitan Area (CMA) and Census Tract (CT) definition. URL: http://www.geog.ubc.ca/metropolis/atlas/Introduction/Definitions/definitions.htm, (last date accessed: 2 June 2004).

ERDAS, 2003. *ERDAS Field Guide,* 7/e, Leica Geosystems GIS & Mapping, LLC, U.S.A. 698p.

Fisher, P.F. and C. Pathirana, 1990. The Evaluation of Fuzzy Membership of Land Cover Classes in the Suburban Zone. *Remote Sensing of Environment,* 34 (2): 121-132.

Foody, G. M., M. B. McCulloch and W. B. Yates, 1995. Classification of Remotely Sensed Data by An Artificial Neural Network: Issues Related to Training Data Characteristics. *Photogrammetric Engineering and Remote Sensing,* 61(4): 391-401.

Forster, B.C., 1980. Urban Residential Ground Cover Using Landsat Digital Data. *Photogrammetric Engineering and Remote Sensing,* 46 (3): 547-558.

Forster, B.C., 1983. Some Urban Measurements from Landsat Data. *Photogrammetric Engineering and Remote Sensing,* 49(12): 1693-1707.

Forster, B.C., 1985. An Examination of Some Problems and Solutions in Monitoring Urban Areas from Satellite Platforms. *International Journal of Remote Sensing,* 6(1):139-151.

Forster, B.C., 1993. Coefficient of Variation as a Measure of Urban Spatial Attributes Using SPOT HRV and Landsat TM Data. *International Journal of Remote Sensing.* 14(12): 2403–2409.

Forsythe, K.W., 2004. Pansharped Landsat 7 Imagery for Improved Urban Area Classification. *Geomatica,* 58(1): 23-31

Fung, T. and E. LeDrew, 1988. The Determination of Optimal Threshold Levels for Change Detection Using Various Accuracy Indices. *Photogrammetric Engineering and Remote Sensing,* 54(10): 1449-1454.

Gamba, P., J.A. Banediktsson and D. Wilkinson, 2003. Foreword to the Special Issue on Urban Remote Sensing by Satellites. *IEEE Transactions on Geoscience and Remote Sensing,* 40(9): 1903-1906.

GeoCommunity, 2004. Sensor Description... QuickBird, URL: http://imaging.geocomm. com/features/sensor/quickbird/, (last date accessed: 20 May 2004).

Gillespie, A.R., M.O. Smith, J.B. Adams, S.C. Willis, A.F. Fischer and D.E. Sabol, 1990. Interpretation of Residual Images: A Spectral Mixture Analysis of AVIRIS Images. Proceedings of the Second Airborne Visible/Infrared Imaging Spectrometer (AVIRIS) Workshop, 4-5 June 1990, Pasadena, CA, (R. Green, editor), JPL publication, No. 90-45, pp. 243-270.

Gluch, R., 2002. Urban Growth Detection Using Texture Analysis on Merged Landsat TM and SPOT Data. *Photogrammetric Engineering and Remote Sensing,* 68 (12): 1283-1288.

Gomarasca, M. A., P. A. Brivio, F. Pagnoni and A.Galli, 1993. One Century of Land Use Changes in the Metropolitan Area of Milan (Italy). *International Journal of Remote Sensing,* 14(2): 211–223.

Gong, P. and P.J. Howarth, 1990. The Use of Structural Information for Improving Land-Cover Classification Accuracies at the Rural-urban Fringe. *Photogrammetric Engineering and Remote Sensing,* 56(1): 67-73.

Gong, P., and P.Howarth, 1992. Land-use Classification of SPOT HRV Data Using a Cover-frequency Method. *International Journal of Remote Sensing,* 13(8): 1459–1471.

Gong, P., 1993. Change Detection Using Principal Component Analysis and Fuzzy Set Theory. *Canadian Journal of Remote Sensing,* 19(1): 22–29.

Green, K., D. Kempka and L. Lackey, 1994. Using Remote Sensing to Detect and Monitor Land-cover and Land-use Change. *Photogrammetric Engineering and Remote Sensing,* 60(3): 331–337.

Griffith, J. A., S. V. Stehman, T. L. Sohl and T. R. Loveland, 2003. Detecting Trends in Landscape Pattern Metrics Over a 20-year Period Using a Sampling-based Monitoring Programme. *International Journal of Remote Sensing,* 24 (1): 175-181.

Haack, B., N. Bryant and S. Adams, 1987. An Assessment of Landsat MSS and TM Data for Urban and Near-urban Land-cover Digital Classification. *Remote Sensing of Environment,* 21(2): 201–213.

Harris, R., 1985. Contextual Classification Post-processing of Landsat Data Using a Probabilistic Relaxation Model. *International Journal of Remote Sensing,* 6(6): 847-866.

Harris, P. M., and S. J. Ventura, 1995. The Integration of Geographic Data with Remotely Sensed Imagery to Improve Classification in an Urban Area. *Photogrammetric Engineering and Remote Sensing,* 61(8): 993–998.

Herold, M., S. Liu and K.C. Clarke, 2003. Spatial Metrics and Image Texture for Mapping Urban Land Use. *Photogrammetric Engineering & Remote Sensing,* 69 (9): 991-1001.

Hung, M.-C., 2001. Using the V-I-S Model to Analyze Urban Environment from TM Images. *Proceedings of URISA 2001 Annual Conference*, 20-24 October 2001. Long Beach, CA.

Imhoff, M., W. Lawerence, D. Stutzer and C. Elvidge, 1997. A Technique for Using Composite DMSP/OLS 'City Lights' Satellite Data to Map Urban Area. *Remote Sensing of Environment,* 61(3): 361–370.

Industry Canada, 2004. Mississauga, Ontario, URL: http://broadband.gc.ca/demographic_servlet/community_demographics/2872, (last date accessed: 29 May 2004).

Infoterra, 2004. SPOT, URL: http://www.infoterra-global.com/spot.htm, (last date accessed: 20 May 2004).

Jackson, M.J., P. Carter, T.F. Smith and W. Gardner, 1980. Urban Land Mapping from Remotely-sensed Data. *Photogrammetric Engineering and Remote Sensing,* 46(8): 1041-1050.

Jensen, J.R., 1981. Urban Change Detection Mapping Using Landsat Data. *The American Cartographer,* 8(2): 127-147.

Jensen, J.R., 1983. Urban/suburban Land Use Analysis, *Manual of Remote Sensing* (R.N. Colwell, editor), *2/e,* Falls Church, Virginia: ASPRS, pp. 1571-1666.

Jensen, J.R., 1996. *Introductory Digital Image Processing: A Remote Sensing Perspective*, 2/e. Prentice-Hall, Upper Saddle River, New Jersey, 316p.

Lambin, E.F. and A.H. Strahler, 1994a. Change –vector Analysis in Multispectral Space: A Tool to Detect and Categorize Land-cover Change Processes Using High Temporal-resolution Satellite Data. *Remote Sensing of Environment,* 48 (2): 231-244.

Langford, M., D.J. Maguire and D.J. Unwin, 1991. The Areal Interpolation Problem: Estimating Population Using Remote Sensing in a GIS Framework, *Handling Geographic Information* (I. Masser and M. Blakemore, editors), Longman, London, pp. 55-77.

Langford, M. and D.J. Unwin, 1994. Generating and Mapping Population Density Surfaces within a Geographical Information System. *The Cartographic Journal,* 31(1): 21-26.

Li, J. and H.M. Zhao, 2004. Detecting Urban Land-use and Land-cover Changes in Mississauga Using Landsat TM Images. *Journal of Environmental Informatics,* 2 (1): 38-47.

Lillesand, T.M., R.W. Kiefer and J.W. Chipman, 2004. *Remote Sensing and Image Interpretation,* 5/e, John Wiley & Sons, New York, NY, 763p.

Lillesand, T.M. and R.W. Kiefer, 2000. *Remote Sensing and Image Interpretation, 4*/e, John Wiley & Sons, Inc., New York, NY, 208p.

Liu, X.-H., A. K. Skidmore and H. Van Oosten, 2002. Integration of Classification Methods for Improvement of Land-cover Map Accuracy. *ISPRS Journal of Photogrammetry & Remote Sensing,* 56(4): 257-268.

Lo, C.P., 1995. Automated Population and Dwelling Unit Estimation from High-resolution Satellite Images: A GIS Approach. *International Journal of Remote Sensing.* 16(1): 17-34.

Lo, C. P., 1997. Application of Landsat Thematic Mapper Data for Quality of Life Assessment in an Urban Environment. *Computers, Environment and Urban Systems,* 21 (3/4): 259–276.

Lo, C. P. and B.Faber, 1997. Integration of Landsat Thematic Mapper and Census Data for Quality of Life Assessment. *Remote Sensing of Environment.* 62 (2): 143–157.

Lo, C.P., 2001. Modeling the Population of China using DMSP Operational Linescan System Nighttime Data, *Photogrammetric Engineering and Remote Sensing,* 67(9): 1037-1047.

Lunetta, R.S., 1999. Applications, Project Formulation, and Analytical Approach, *Remote Sensing Change Detection-Environmental Monitoring Methods and Application* (R.S. Lunetta, and C.D. Elvidge, editors), Taylor & Francis, London. pp. 1-19.

Madhavan, B.B., S. Kubo, N. Kurisaki and T.V.L.N. Sivakumar 2001. Appraising the Anatomy and Spatial Growth of the Bangkok Metropolitan Area using a Vegetation-impervious-soil model through Remote Sensing. *International Journal of Remote Sensing,* 22(5): 789-806.

Markham, B. L., and R. G. Townshend, 1981. Land Cover Classification Accuracy as a Function of Sensor Spatial Resolution. In *Proceedings of the Fifteenth International Symposium on Remote Sensing of Environment,* May 1981, Ann Arbor, Michigan, *pp.* 1075–1085.

Martin, L. R. G., and P. J. Howarth, 1989. Change Detection Accuracy Assessment Using SPOT Multispectral Imagery of the Rural-urban Fringe. *Remote Sensing of Environment,* 30 (1): 55- 66.

Martin, L. R. G., and P. J. Howarth, 1988. Multispectral Classification of Land Use at the Rural-urban Fringe Using SPOT Data. *Canadian Journal* of *Remote Sensing,* 14 (2): 55- 66.

Mesev, V., B. Gorte and P.A. Longley, 2001. Modified Maximum-Likelihood Classification Algorithms and their Application to Urban Remote Sensing, *Remote Sensing and Urban Analysis*, (J.P. Donnay, M.J. Barnsley and P.A. Longley, editors), Taylor & Francis, London, pp. 71-88.

Mokken, R.J., 1995. Remote Sensing, Statistics and Artificial Neural Networks, URL: http://ltpwww.gsfc.nasa.gov/ISSSR-95/remotes3.htm, (last date accessed: 26 May 2004).

Møller-Jensen, L., 1990. Knowledge-Based Classification of an Urban Area Using Texture and Context Information in Landsat-TM Imagery. *Photogrammetric Engineering and Remote Sensing,* 56(6): 899-904.

Nellis, M.D., K. Lulla and J. Jensen, 1990. Interfacing Geographic Information Systems and Remote Sensing for Rural Land-use Analysis. *Photogrammetric Engineering and Remote Sensing,* 56 (3): 329-331.

Nelson, R.F., 1983. Detecting Forest Canopy Change Due to Insect Activity Using Landsat MSS. *Photogrammetric Engineering and Remote Sensing,* 49 (9): 1030-1314.

Onsi, H. M., 2003. Designing a Rule-based Classifier Using Syntactical Approach. *International Journal of Remote Sensing,* 24(4): 637-647.

Pathan, S.K., S.V.C. Sastry, P.S. Dhinwq, M. Rao, M.K. L., S. Kumar, V.N. Patkar and V.N. Phatak, 1993. Urban Growth Trend Analysis Using GIS Techniques – a case study of the Bombay Metropolitan Region. *International Journal of Remote Sensing,* 14 (17): 3169-3179.

PCI Geomatics, 2004. Pan sharpening, URL: http://www.pcigeomatics.com/support_center/quickguides/pansharp.pdf, (last date accessed: 1 Jan. 2004).

Pedroni, L., 2003. Improved classification of Landsat Thematic Mapper Data Using Modified Prior Probabilities in Large and Complex Landscapes. *International Journal of Remote Sensing,* 24(1): 91-113.

Peel, 2004. The Social Planning Council of Peel, URL: http://www.spcpeel.com/Pub_InfoShare_July2002.asp, (last date accessed: 25 January 2004).

Phinn, S., M.Stanford, P. Scarth, A.T. Murry and P.T. Shyy, 2002. Monitoring the Composition of Urban Environments Based on the Vegetation-Impervious surface-Soil (VIS) Model by Subpixel Analysis Techniques. *International Journal of Remote Sensing,* 23(20): 4131-4153.

Pozzi, F. and C. Small, 2002. Vegetation and Population Density in Urban and Suburban Areas in the U.S.A. *Paper Presented at the 3rd International Symposium on Remote Sensing of Urban Areas,* Istanbul, Turkey, June 2002.

Qiu, F., K.L. Woller and R. Briggs, 2003. Modeling Urban Population Growth from Remotely Sensed Imagery and TIGER GIS Road Data. *Photogrammetric Engineering and Remote Sensing,* 69 (9): 1031-1042.

Ranchin, T., L. Wald and M. Mangolini, 2001. Improving the Spatial Resolution of Remotely-Sensed Images by Means of Sensor Fusion: A General Solution Using the ARISIS Method, *Remote Sensing and Urban Analysis*, (J.P. Donnay, M.J. Barnsley and P.A. Longley, editors), Taylor & Francis, London, pp. 21-37.

RADARSAT International, 2004. Products & Pricing, URL: http://www.rsi.ca/products/index_products.asp, (last date accessed: 5 July 2004).

Ridd, M.K., 1995. Exploring a V-I-S (Vegetation-impervious-soil) Model for Urban Ecosystem Analysis through Remote Sensing: Comparative Anatomy for Cities. *International Journal of Remote Sensing,* 16(12): 2165-2185.

RST, 2004. Section 4-Urban and Land Use Applications, URL: http://rst.gsfc.nasa.gov/Sect4/Sect4_1.html, (last date accessed: 22 May 2004).

Shackelford, A.K. and C.H. Davis, 2003. A Hierarchical Fuzzy Classification Approach for High-Resolution Multispectral Data over Urban Areas. *IEEE Transactions on Geoscience and Remote Sensing,* 41(9): 1920-1932.

SIMWRIGHT, 2004. SPOT Imagery Pricing, URL: http://www.simwright.com/imagery%20pricing/Catalogs/spot/spot%20Pricing.htm, (last date accessed: 5 July 2004).

Singh, A., 1989. Digital Change Detection Techniques Using Remotely-Sensed Data. *International Journal of Remote Sensing,* 10(6): 989-1003.

Statistics Canada, 2004. Geocommunity, URL: http://imaging.geocomm.com/features/sensor/quickbird/, (last date accessed: 20 May 2004).

Statistics Canada: 2001 Census: Population and Dwelling counts, 2004, URL: http://www12.statcan.ca/english/census01/products/standard/popdwell/Table-CMA-C.cfm?CMA=535, (last date accessed: 17 February 2004).

Sutton, P., 1997. Modeling Population Density with Night-time Satellite Imagery and GIS. *Computers, Environment and Urban Systems,* 21(3/4): 227–244.

USGS, 2004. Pricing Information: Aerial Photographs, URL: http://geography.usgs.gov/esic/prices/aerial_photos.html, (last date accessed: 5 July 2004).

Wang, F., 1990. Fuzzy Supervised Classification of Remote Sensing Images. *IEEE Transactions on Geoscience and Remote Sensing,* 28(2): 194-201.

Webster, C.L., W. Oltof and M. Berger, 1991. *Exploring the Discriminating Power of Texture Statistics in Interpreting a SPOT Satellite Image of Harare*, Technical Report in Geoinformation System, Computing and Cartography 36, University of Wales Cardiff, Wales and South West Regional Research Laboratory.

Weismiller, R.A., S.J. Kristof, D.K. Scholz, P.E. Anuta and S.A. Monin, 1977. Change Detection in Coastal Zone Environments. *Photogrammetric Engineering & Remote Sensing,* 43(12): 1533-1539.

Welch, R., 1982. Spatial Resolution Requirements for Urban Studies. *International Journal of Remote Sensing,* 3(2): 139-146.

Welch, R. and W. Ehlers, 1987. Merging Multiresolution SPOT HRV and Landsat TM Data. *Photogrammetric Engineering & Remote Sensing,* 53(3): 301-303.

Weng, Q., 2001. A Remote Sensing–GIS Evaluation of Urban Expansion and Its Impact on Surface Temperature in the Zhujiang Delta, China. *International Journal of Remote Sensing,* 22(10): 1999-2014.

Westmoreland, S. and D.A. Stow. 1992. Category Identification of Changed Land-use Polygons in an Integrated Image Processing/Geographic Information System. *Photogrammetric Engineering & Remote Sensing,* 58(11): 1593-159.

Wilkinson, G.G., 1996. A Review of Current Issues in the Integration of GIS and Remote Sensing Data. *International Journal of Geographical Information Systems,* 10(1): 85-101.

Williams, D. L., J. R. Irons, B. L. Marham, R.F. Markham, R.F. Nelson, D.L. Toll, R.S. Latty and M.L. Stauffer, 1984. A Statistical Evaluation of the Advantages of Landsat Thematic Mapper Data in Comparison to Multispectral Scanner Data. *IEEE Transactions on Geoscience and Remote Sensing.* GE-22: 294–301.

Yang, L., G. Xian, G. Xian, J.M. Klaver and B. Deal, 2003. Urban Land-cover Change Detection through Sub-pixel Imperviousness Mapping Using Remotely Sensed Data. *Photogrammetric Engineering & Remote Sensing,* 69(9): 1003-1010.

Yang, X. and C. P. Lo, 2002. Using a Time Series of Satellite Imagery to Detect Land Use and Land Cover Changes in the Atlanta, Georgia Metropolitan Area. *International Journal of Remote Sensing,* 23 (9): 1775-1789.

Yang, X., 2003. Remote Sensing and GIS for Urban Analysis: An Introduction. *Photogrammetric Engineering & Remote Sensing,* 69(9): 937.

Yuan, Y., R.M. Smith and E.F. Limp, 1997. Remodeling Census Population with Spatial Information from Landsat TM Imagery. *Computers, Environment and Urban Systems,* 21(3/4): 245-258.

Zhang, Y., 1999. A New Method for Merging Multispectral and Mutliresolution Satellite Data and its Spectral and Spatial Effects. *International Journal of Remote Sensing,* 20 (10): 2003-2014.

Zhang, Y., 2002. A New Automatic Approach for Effectively Fusing Landsat 7 and IKONOS Images. *IEEE/IGARSS'02,* Toronto, Canada. June 24-28, 2002.